Distribution Category UC-95e

FINAL TECHNICAL REPORT

COthane, METHANE FROM WASTE CO

J. A. Rabo, and A. C. Frost,
L. F. Elek, A. P. Risch, C-L. Yang

Union Carbide Corporation
Tarrytown Technical Center
Old Saw Mill River Road
Tarrytown, New York 10591

Date Published - December, 1980

Prepared for the United States
Department of Energy
Office of Industrial Programs

Under Contract No.
DE-AC03-78CS40177

ABSTRACT

As the result of early efforts in the fields of catalysis, coal gasification, and methanation, Union Carbide developed a novel process for the direct concentration and conversion of CO in dilute waste streams to high quality methane (SNG). This two bed, two step process was dubbed COthane, a contraction of the feed carbon monoxide (CO) and the product methane.

The objectives of this contract was to develop the COthane process up to the large pilot plant stage, to develop an improved catalyst, and to estimate the cost of methane produced by this process.

The process development studies yielded all of the design parameters required to design a large scale pilot plant, the catalyst development program produced a catalyst with promising stability, and the economic studies showed that methane production cost would generally be more than $6/MM BTU.

Because this cost is above those for natural gas, further work on this project has been suspended until rising natural gas prices catch up with the more slowly rising COthane production cost.

TABLE OF CONTENTS

TABLE OF CONTENTS
(continued)

I SUMMARY

Each year large quantities of dilute carbon monoxide in industrial waste streams are flared or vented to the atmosphere. In an effort to recover this wasted source of energy, Union Carbide developed, on a laboratory scale, the COthane process for the direct conversion of the dilute carbon monoxide in such streams to pipeline quality natural gas (SNG).

During the first step of this two step, multi-bed process, the waste gas is passed over a bed of catalyst where the carbon monoxide disproportionates into ejected carbon dioxide and deposited active carbon. During the second step, moderate pressure steam reacts with the active carbon to form methane and carbon dioxide. Removal of the carbon dioxide and residual water yields pipeline quality SNG.

A three phase program was planned for the commercialization of the COthane process. Phase I, completed and detailed in this report, defined the process parameters. Phase II, not yet started, would further test the process with an integrated pilot unit operating on industrial waste streams. Phase III would monitor the operation of the first commercial unit.

The primary purpose of DOE contract DE-AC03-78CS40177, which ran from 25 September 1978 to 31 December 1980, was to carry out the Phase I effort. This effort covered bench scale pilot runs, the development of an improved catalyst, and technical-economic studies. The purpose of this Final Technical Report is to describe the work done in these areas during the course of the contract.

The bench scale pilot plant runs yielded the reaction zone lengths, heat dissipation requirements, production rates, and reactant utilizations, required to size and cost a commercial system and to supply the design parameters for the Phase II pilot plant. New catalysts developed with different matrixing agents, metal components, stabilizing agents, and synthesis techniques showed a promising degree of stability. Finally, the technical and economic studies showed that, under certain conditions, the COthane production costs (in mid-1980 dollars) are $5.78/MM BTU for blast furnace off-gas, $7.11/MM BTU for basic oxygen furnace off-gas, and $6.00 to $8.10/MM BTU for carbon black off-gas.

Recent market surveys, carried out by Union Carbide Corporation, have indicated that there is no longer a surplus of blast furnace off-gas available for the COthane process, and that the basic oxygen furnace off-gas and carbon black off-gas applications are promising only if the COthane production costs are competitive with the current $2-$4/MM BTU price for natural gas.

The magnitude of the difference between the COthane production costs and the current price for natural gas suggests that all work on the COthane process should be temporarily suspended. Because the cost of the COthane process will increase less rapidly than the cost of the fuel, and because a reasonable increase in catalyst performance will have a significant effect on reducing COthane costs, an additional catalyst development effort would be appropriate at some future time when fuel costs have risen substantially above their present levels. Such an additional catalyst development effort would preceed the Phase II pilot plant studies.

The objectives of this contract, to define the basic design parameters of the COthane process, have been achieved. Sufficient technical, economic and marketing data were obtained to conclude that the program should be temporarily suspended, be re-examined in a few years, and then possibly be resumed at that time with an additional catalyst development effort prior to the commencement of the Phase II pilot plant studies.

II INTRODUCTION

BACKGROUND

Table I, compiled from data given in a 1976 survey (31), shows that as much as 24 million tons/yr. of dilute carbon monoxide are probably being wastefully flared or vented to the atmosphere by steel mills, foundries, oil refineries, and carbon black plants. This is the energy equivalent of about 570 million cubic feet/day of natural gas. Until now, no economical means of recovering this energy has existed. The dilute carbon monoxide would first have to be separated and then reacted with hydrogen to convert it to useful methane fuel. The cost of these routine processes of concentration and methanation are presently greater than the value of the energy recovered.

Union Carbide has been working for several years in the fields of catalysis, coal gasification, methanation and related research. As a result of these efforts, a novel process was developed, on a laboratory scale, for the direct concentration and conversion of carbon monoxide in dilute streams to high quality methane (SNG) at a cost believed to be competitive with natural gas (33). This new process was dubbed COthane—a contraction of the feed carbon monoxide (CO) and the product methane.

TABLE 1

SUMMARY OF DILUTE CO SOURCES AND METHANE POTENTIAL

CO SOURCE (% CO)	AVAILABLE CO[1] (MM TONS/YR)	METHANE POTENTIAL BY COthane (SCFD)
BLAST FURNACE GAS (22-26%)	12.40	250
BOF[2] (54-68%)	4.10	82
GRAY IRON CASTING (15%)	1.30	26
ALUMINUM PRODUCTION (30%)	0.24	5
CARBON BLACK MFG (6-9%)	2.28	45
PETROLEUM REFINING (8%)	3.60	72
IN-SITU GASIFICATION[3] (15%)	0.55	11
TOTAL	24.47 MM TONS/YR	491 MM SCFD

(1) ONLY CO FLARED OR EXHAUSTED IS CONSIDERED (31).

(2) AT BOF VESSEL MOUTH (BEFORE COMBUSTION): A CONSERVATIVE ESTIMATE.

(3) PROJECTED HANNA IV LEVELS.

THE COTHANE PROCESS

The COthane process (1) for the carbon monoxide-to-methane conversion is a two-step, multiple reactor system. Figure 1 shows that during the first step the waste gas is appropriately pretreated, preheated, and passed through the first reactor containing a bed of nickel or cobalt catalyst. At ~270-300°C the catalyst causes the carbon monoxide in the stream to disproportionate into CO_2 and an active carbon species, C*. The CO_2 is carried out of the reactor along with the diluents in the waste gas. The active carbon is deposited at the surface of the catalyst. This first step can be expressed as:

$$4CO \xrightarrow[\text{Ni,Co}]{270\text{-}300^{\circ}C} 2CO_2 + 2C^* \qquad (1)$$

This reaction continues in the first reactor until most of the catalyst has been loaded with active carbon. The waste gas is then diverted to a second reactor containing catalyst which has been stripped of its previously accumulated carbon. Moderate pressure steam is simultaneously introduced into the first reactor where it reacts with the active carbon to form methane and carbon dioxide. This second step can be expressed as:

$$2C^* + 2H_2O \xrightarrow[\text{Ni,Co}]{270\text{-}300^{\circ}C} CH_4 + CO_2 \qquad (2)$$

This reaction continues in the first reactor until all of the active carbon has been removed from the catalyst. The duration of this step is the same as that of the first step, so that upon its completion the waste gas will be switched back from the second reactor to the first reactor. This cycle continuously repeats itself.

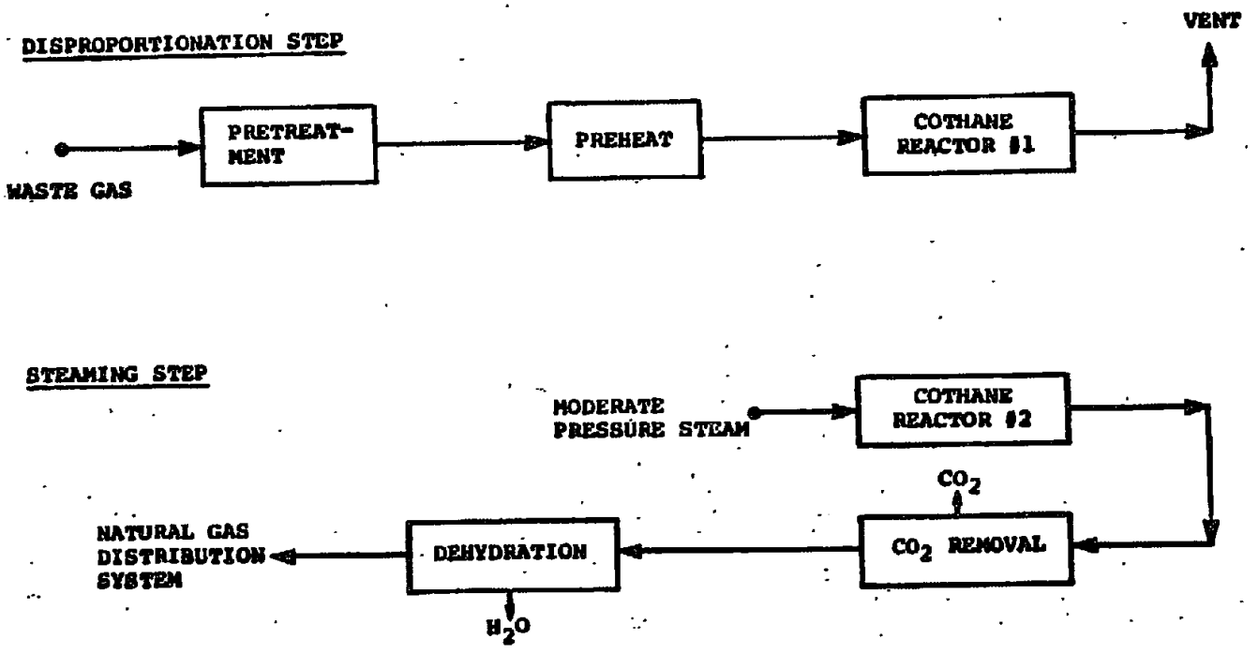

FIGURE 1

SCHEMATIC DIAGRAM FOR THE COTHANE PROCESS

The wet CO_2 and methane stream produced from the second step is treated to remove the carbon dioxide and water, so that the remaining high quality methane may be piped into the local natural gas distribution system.

The feed pretreatment step shown in Figure 1 will depend on the nature of the constituents in the feed gas. If the feed gas contains oxygen, it will react with the active carbon as quickly as it is formed to produce carbon dioxide. In addition to lowering the overall efficiency of the conversion of the waste carbon monoxide to recoverable methane, this oxidation reaction is highly exothermic and will increase the cooling requirements for the already highly exothermic disproportionation step. Consequently, the oxygen level should be kept to some reasonable fraction of the carbon monoxide content before the feed gas is sent to the COthane reactors, presumably with a pre-oxidation step. Other reactive diluents in the feed gas, such as water vapor and hydrogen, can also be expected to react with the active carbon as it is formed. However, the actual effects of these reactants on the formation of active carbon at the disproportionation step conditions is negligible for water and helpful for hydrogen, as is shown in Chapter IV.

The feed gas should also be treated to remove catalyst poisons. Hydrogen sulfide, for instance, requires the use of not only a preliminary treatment step, such as an amine scrubber, but the use of a zinc oxide guard bed as well.

During each of the COthane process cycles described above, there will be a small fraction of carbon formed during the disproportionation step that will not be removed during the steaming step. This "inactive" carbon will slowly build up as the number of cycles increases, until its presence on the catalyst hinders the efficiency of the cycle. When the methane production rate drops to a minimum allowable level, the reactor containing this inhibited catalyst is withdrawn from service and subjected to a carbon removal step. This "regeneration" step is usually carried out with a low concentration (~½ vol.%) oxygen stream at a 400°C initiation temperature; when all of the carbon has been oxidized in this manner, the catalyst is then subjected to a hydrogen-containing stream so that the nickel oxide formed during the oxidation step is reduced back to nickel.

Combining the disproportionation step reaction (Reaction 1) with the steaming step reaction (Reaction 2) yields the overall COthane reaction,

$$4CO + 2H_2O \rightleftharpoons CH_4 + 3CO_2 \qquad (3)$$

Four volumes of carbon monoxide produce one volume of methane. Since one volume of methane has 3.15 times the gross heat of combustion of one volume of carbon monoxide, 78.7% of the gross energy available in the original carbon monoxide remains in the product methane {(3.15)(100)/(4) = 78.7%}.

The flow scheme for the cyclic COthane process not only has the operating simplicity of the commercial pressure-swing adsorption processes, but, simplistically, it performs the separation of carbon monoxide from its diluents and the subsequent conversion of that CO to moderate pressure methane in a single reactor, without the need for the standard, expensive steps of CO concentration, steam shifting, methanation, and tail gas compression. Consequently, the COthane process is potentially a relatively uncomplicated and inexpensive way to transform waste carbon monoxide into pipeline quality natural gas.

THE COTHANE PROGRAM

The COthane program was divided into three phases. Phase I, completed and detailed in this report, defined the basic process details, including design parameters, and the preferred catalyst composition. Phase II, not yet started, would prove out the results of Phase I in an integrated pilot unit operating on industrial gases. The engineering data from Phase II would be used to design the first commercial unit under Phase III.

The primary purpose of DOE contract DE-AC03-78CS40177, which ran from 25 September 1978 to 31 December 1980, was to carry out the Phase I effort of developing the COthane process to the point where it was ready to be demonstrated on a large scale process development unit (PDU). This Phase I effort was broken down into five tasks.

Tasks 1 and 2 called for the construction and operation of a miniature process development unit (mini PDU) to determine the process variables and efficiencies of the COthane process steps for the most promising catalysts, using both a simple CO/N_2 mixture (Task 1) and more complex synthetic feed streams (Task 2). This mini PDU reactor was of a type that insured approximate design data for the type of commercially-sized reactor envisioned from the studies done as part of Tasks 4 and 5. It should be realized that, because of its small size, this mini PDU reactor yielded basic design data for a commercial reactor that would undoubtedly need to be confirmed by runs on a large-scale PDU reactor, during Phase II.

Task 3 called for the development of catalysts having higher efficiencies, greater stabilities, and superior physical properties than the catalysts previously developed by Union Carbide.

Task 4 called for a technical feasibility study of the various reactor configurations required for carrying out the two exothermic steps of the COthane process in a commercially-sized unit.

Task 5 called for the costing of these different possible reactor configurations to determine the most economically and technically attractive design. The mini PDU reactor used in Tasks 1 and 2 was designed to reflect, as closely as possible for a small-scale laboratory reactor, the behavior of the chosen commercial unit. These technical and economic analyses were continually updated as experimental data became available.

The results obtained for these five Tasks are described in Chapters III, IV, V, VI, and VII, respectively, of this Final Technical Report.

III MINI PDU RUNS WITHOUT REACTIVE DILUENTS

Once the preliminary technical and economic studies, described in Chapters VI and VII, indicated that a tubular reactor held the most promise for a commercial success, a bench-scale process development unit (PDU) was built to imitate the envisioned commercial design as closely as was practical. Runs were made on this unit with a simple CO/N_2 feed stream to yield the following design parameters: i) The effectiveness of heat dissipation from the two process steps, ii) The lengths of the two reaction zones for the two process steps, iii) The methane production rate, iv) The CO utilization, v) The steam utilization, and vi) The extent to which other, ancillary reactions may occur.

DESCRIPTION OF THE UNIT

Figure 2 shows the flow diagram for the mini PDU unit. During the disproportionation step the synthetically blended feed gas is passed successively through a preheat coil, the reactor, a cooler/condenser, a separator, a back pressure regulator, and a gas meter. At the end of the disproportionation step, the CO flow is stopped and the remaining N_2 flow is diverted from the reactor to the vent line. The reactor is then pressurized to the desired steaming pressure with another nitrogen line (not shown), and the steam flow, which has been by-passed through a condenser and a back pressure regulator during the disproportionation step, is routed to the reactor. After a sufficient amount of steam has been fed into the reactor

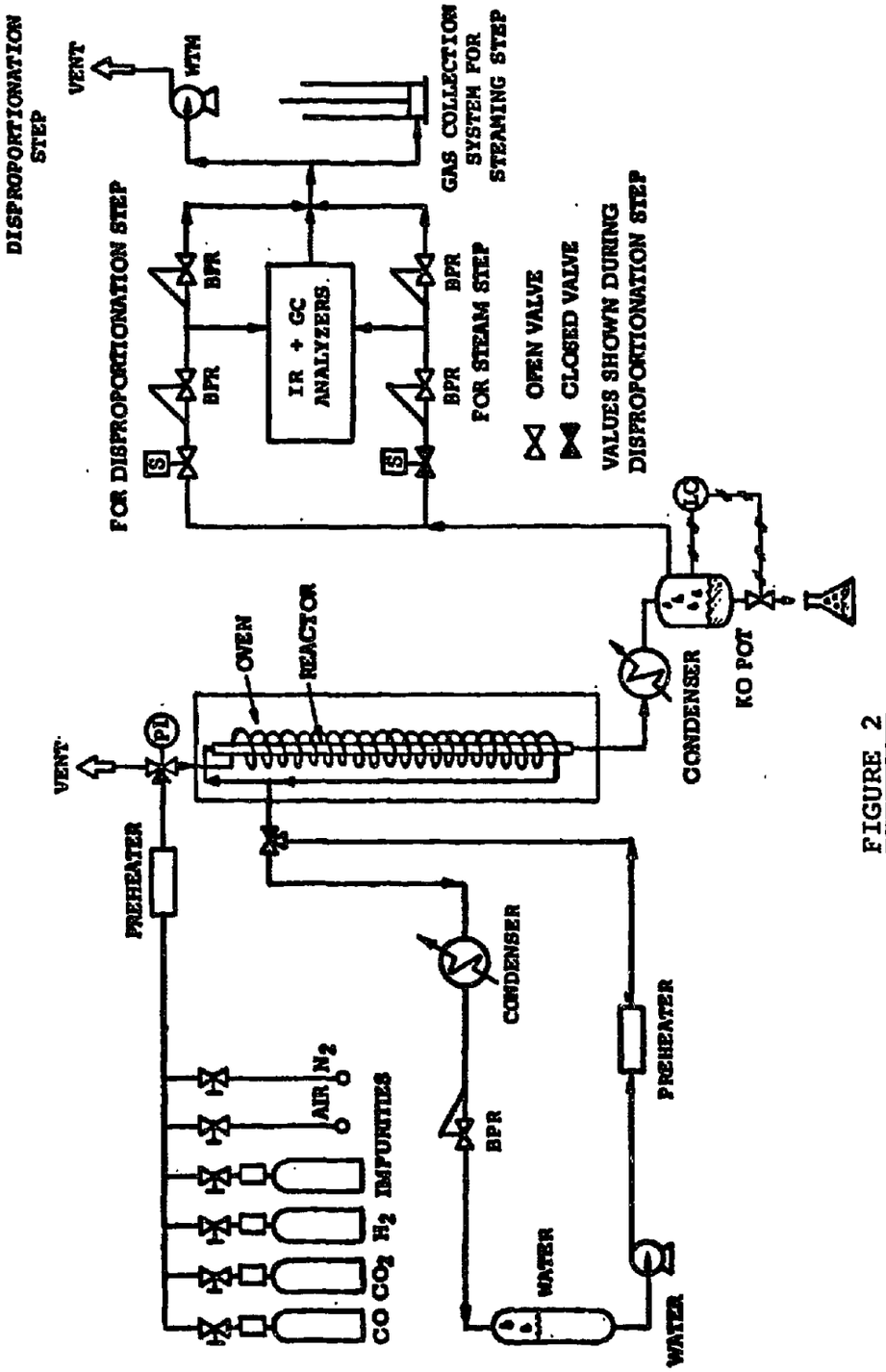

FIGURE 2

FLOW DIAGRAM FOR THE MINI PDU SYSTEM

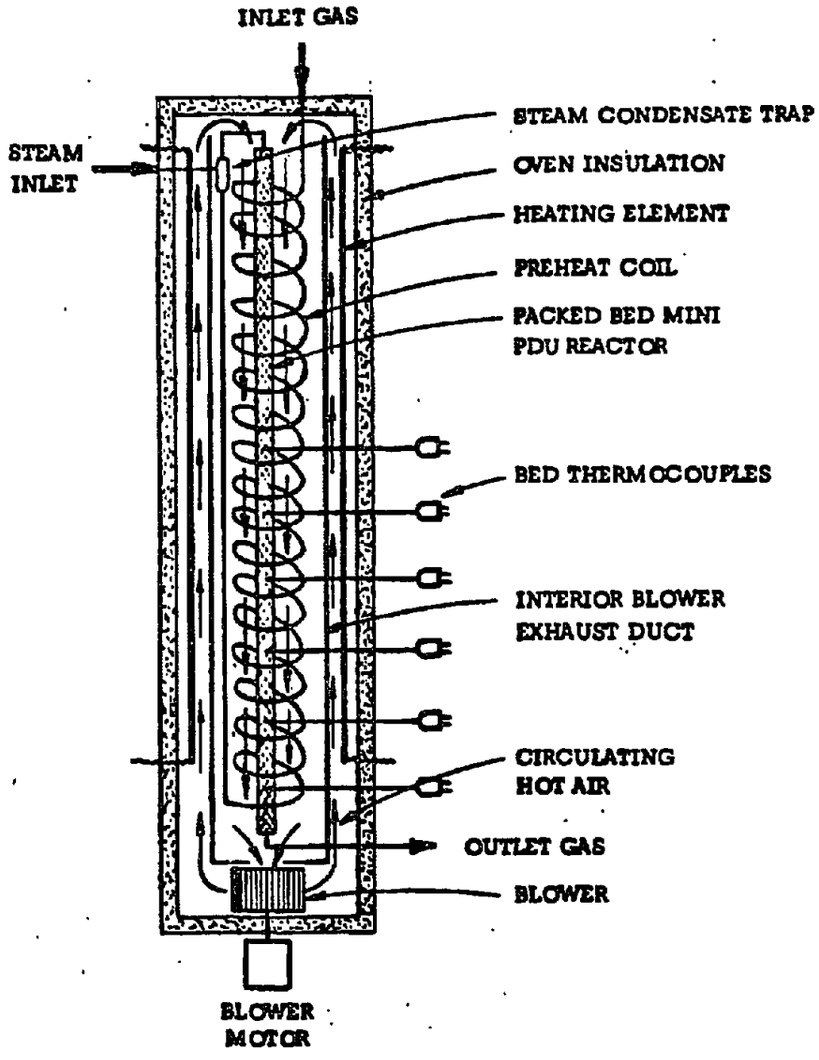

FIGURE 3

MINI PDU REACTOR AND CIRCULATING HOT AIR OVEN

at the desired steaming pressure, the steam flow is again by-passed around the reactor, and the reactor is depressurized in preparation for the next disproportionation step. The CH_4/CO_2/N_2/H_2O effluents from the steaming and depressurization steps pass through the condenser/cooler, the knockout pot, and either a second back pressure regulator for the steaming step, or a by-pass valve for the depressurization step.

The disproportionation feed and effluent streams were monitored continuously with an on stream CO analyzer. The effluents from the steaming and disproportionation steps were either monitored continuously on a spot sample basis with a G.C. analyzer, or they were collected in a large gas collection cylinder and analyzed as a single sample.

The mini PDU reactor itself is a single tube having a diameter and length similar to one of the many such parallel tubes that are incorporated into a commercial tubular reactor. Similarly, the superficial gas velocity, and hence the molar flux, through the tube was also the same as that envisioned for the commercial reactor. Figure 3 shows that the reactor was in a hot circulating air oven. Four additional fans (not shown), mounted horizontally through the two vertical side walls of the oven, insured a high degree of turbulence and temperature uniformity within the interior of the oven.

Initial debugging runs were made with a 1" diameter, 5' long reactor tube and a nickel-zirconia catalyst, which was shown to have in the Chapter V catalyst development studies a high initial

activity and a propensity to form inactive carbon. These characteristics made temperature control difficult for oven temperatures greater than 235°C (14). When the 1" diameter reactor tube was replaced with a 3/4" diameter reactor tube (16), the temperature and mass transfer fronts behaved in the manner anticipated from the Chapter VI reactor studies with an oven temperature at 260-270°C. The runs that were used to obtain design data were made with the more stable nickel-silica catalyst AS-8209-14-22 in 3/4" diameter reactors having five foot and ten foot tube lenghts.

HEAT DISSIPATION

Automatic, cyclic operation of the COthane catalyst AS-8209-14-22 in the 3/4" diameter reactor tubes for cycles as short as 1½ minutes (45 seconds for the disproportionation step and 45 seconds for the pressurization/steaming/depressurization step) showed that the heat dissipation was complete (14, 19, 20), and that the reaction-heating fronts rippled down the tube for the two cyclic steps in the manner predicted by the Chapter VI reactor studies (7). The maximum temperature of these fronts rarely exceeded a desirable 300°C when the oven temperature was 270°C.

The overall heat transfer coefficient for the air-cooled mini PDU reactor tube was found to be 2.8 BTU/ft.^{2}hr.°F, which is considerably lower than the 6-11 BTU/ft.^{2}hr.°F overall heat transfer coefficients expected (23) for a Dowtherm-cooled, 1" diameter, commercial tubular reactor. The Chapter VI reactor studies indicate that such a difference in the overall heat transfer coefficients would probably permit 1" diameter tubes to be used in a commercial reactor.

REACTION ZONE LENGTHS

Early runs with the five foot long reactor tube indicated that the length of the reaction zone for the disproportionation step was still expanding when it reached the end of the tube (17). Since the Chapter VII economic studies indicated that commercial reactor tubes would be 10-15 feet long, most of the mini PDU runs were made with a 10 foot long reactor tube.

Figures 4 and 5 show the extended CO breakthrough curves for three different flowrates at the five foot and ten foot sample taps, respectively. The reaction zone length, calculated (28) from these breakthrough curves, ranged from 3-4 feet for the five foot taps to 6-8 feet for the ten foot taps. Consequently, a properly designed 10 foot long commercial reactor tube would, at the end of the disproportionation step, contain a ~7 foot reaction zone, where the active carbon was still being formed, and a three foot long equilibrium zone, where the active carbon had already formed to the fullest extent possible.

Figures 6 and 7 show how the CO fronts are shortened when the disproportionation step times are reduced from 1 minute to 45 seconds, indicating the development of a shorter equilibrium zone. Similarly, Figures 7 and 8 show how the fronts are further shortened when the feed rate is cut in half during the 45 second disproportionation step, indicating a further shrinkage of the equilibrium zone.

FIGURE 4

EXTENDED CO BREAKTHROUGH CURVES FOR DIFFERENT FEED (25% CO/75% N_2) FLOWRATES WITH THE 3/4" OD REACTOR, A 270°C OVEN TEMPERATURE, A 5 PSIG. EXIT PRESSURE, AND 1/8" EXTRUDATES OF CATALYST NO. AS-8209-14-22 AT THE 5 FOOT TAP

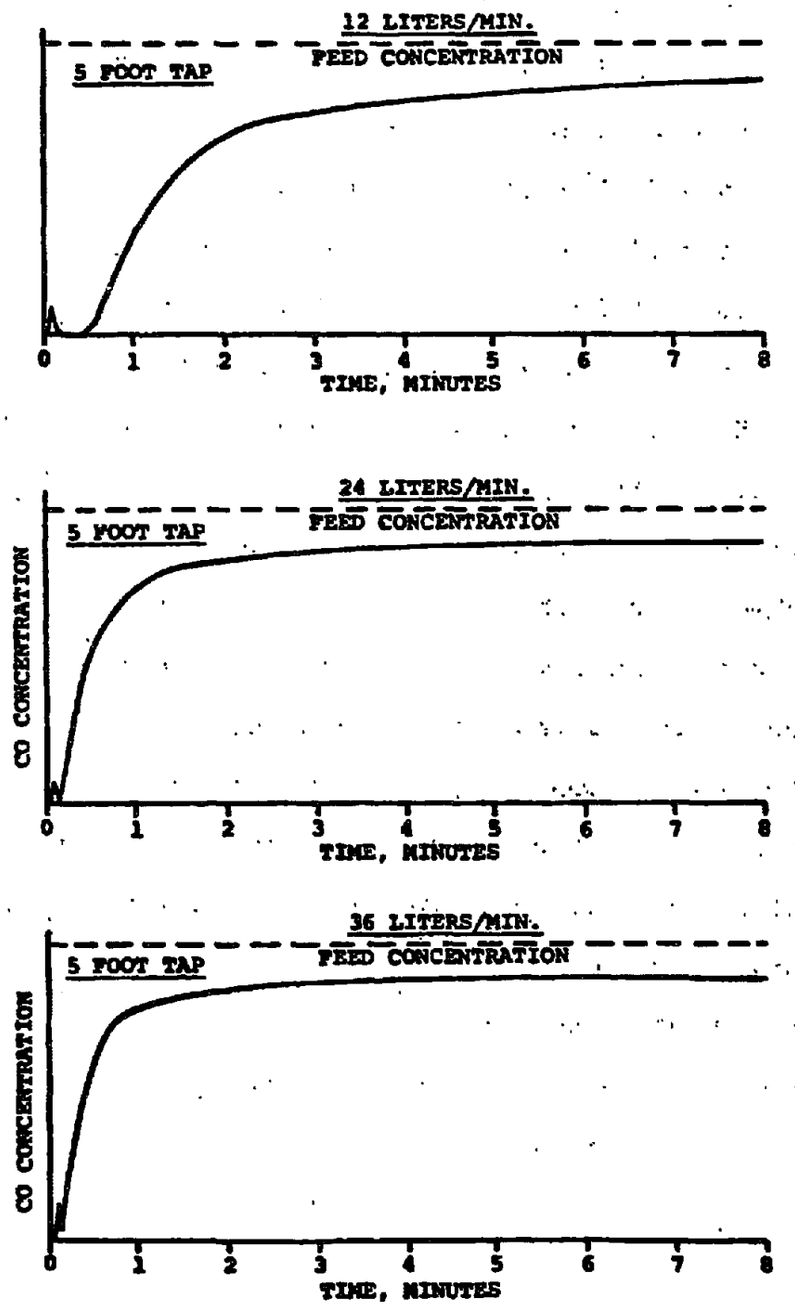

FIGURE 5

EXTENDED CO BREAKTHROUGH CURVES FOR DIFFERENT FEED (25% CO/75% N_2) FLOWRATES WITH THE 3/4" OD REACTOR, A 270°C OVEN TEMPERATURE, A 5 PSIG. EXIT PRESSURE, AND 1/8" EXTRUDATES OF CATALYST NO. AS-8209-14-22 AT THE 10 FOOT TAP

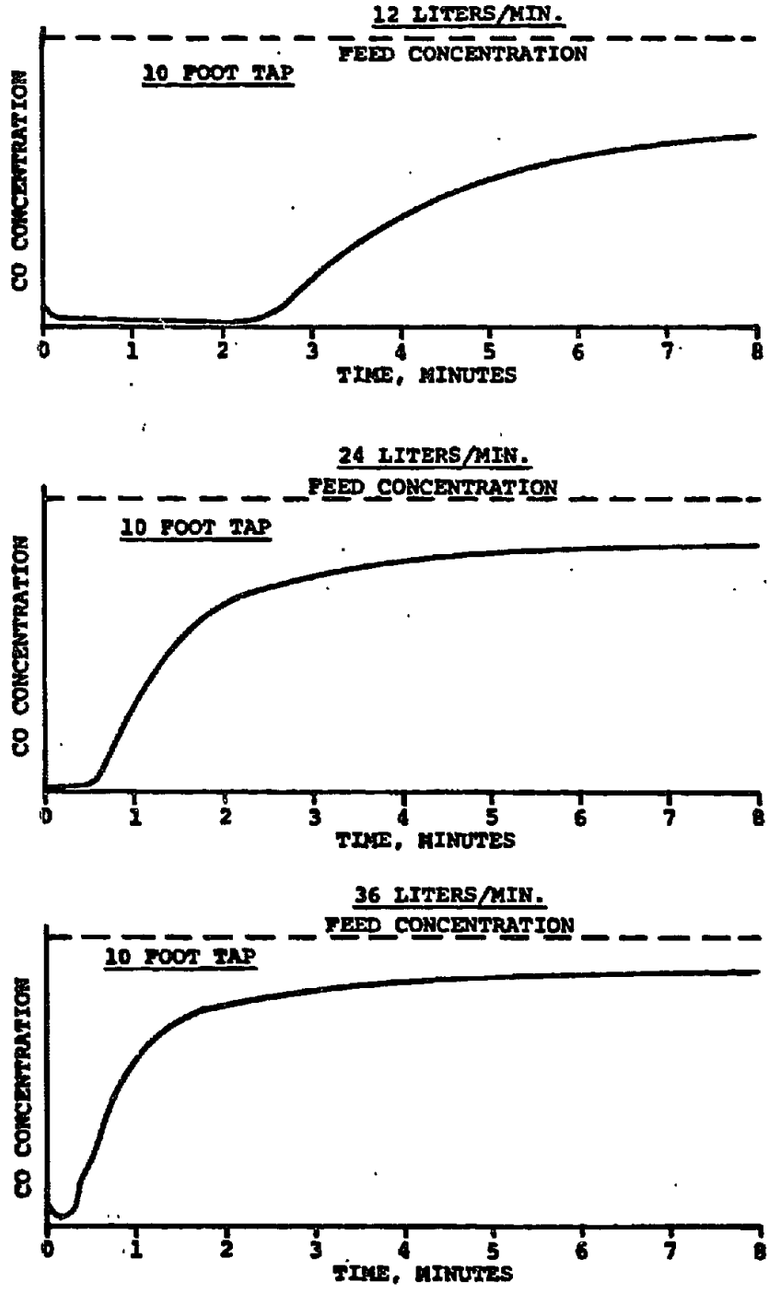

FIGURE 6

CO BREAKTHROUGH CURVES FOR 24 LITERS/MIN. OF 25% CO/75% N_2 DISPROPORTIONATION FEED, A TWO MINUTE CYCLE TIME, A 270°C OVEN TEMPERATURE, A 5 PSIG. EXIT PRESSURE, AND 1/8" EXTRUDATES OF CATALYST NO. AS-8209-14-22

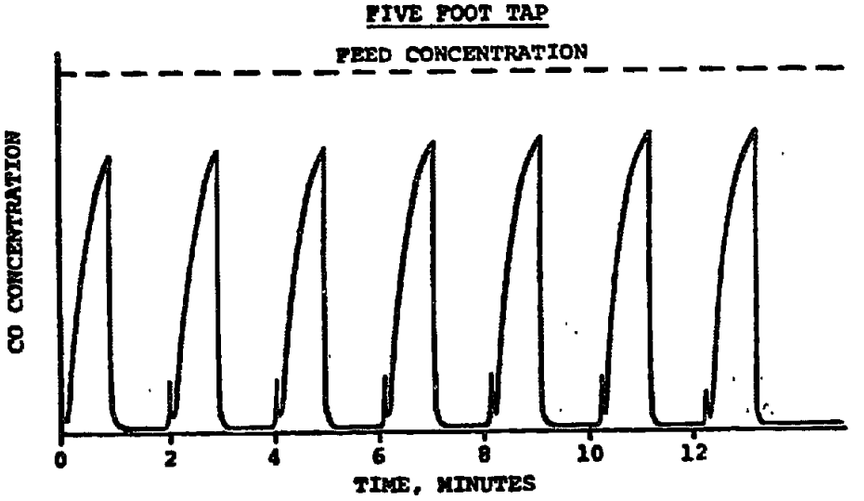

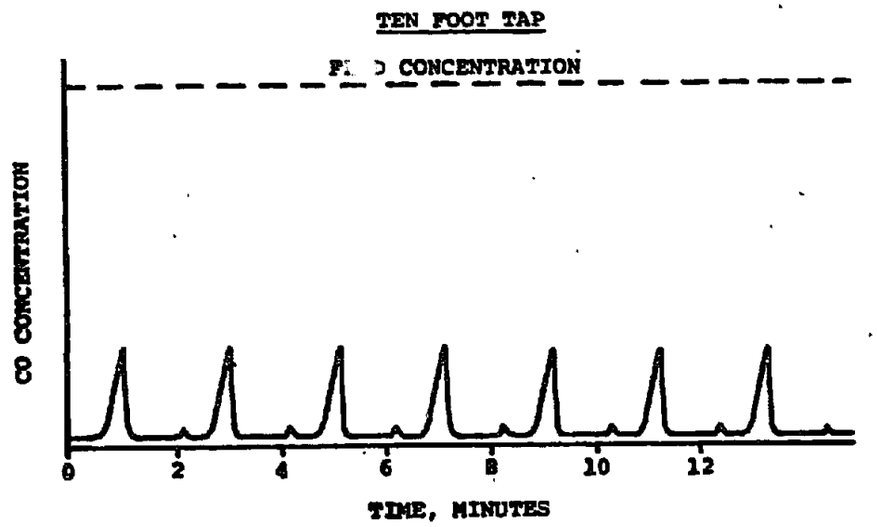

FIGURE 7

CO BREAKTHROUGH CURVES FOR 24 LITERS/MIN. OF 25% CO/75% N_2 DISPROPORTIONATION FEED, A 1½ MINUTE CYCLE TIME, A 270°C OVEN TEMPERATURE, A 5 PSIG EXIT PRESSURE, AND 1/8" EXTRUDATES OF CATALYST NO. AS-8209-14-2

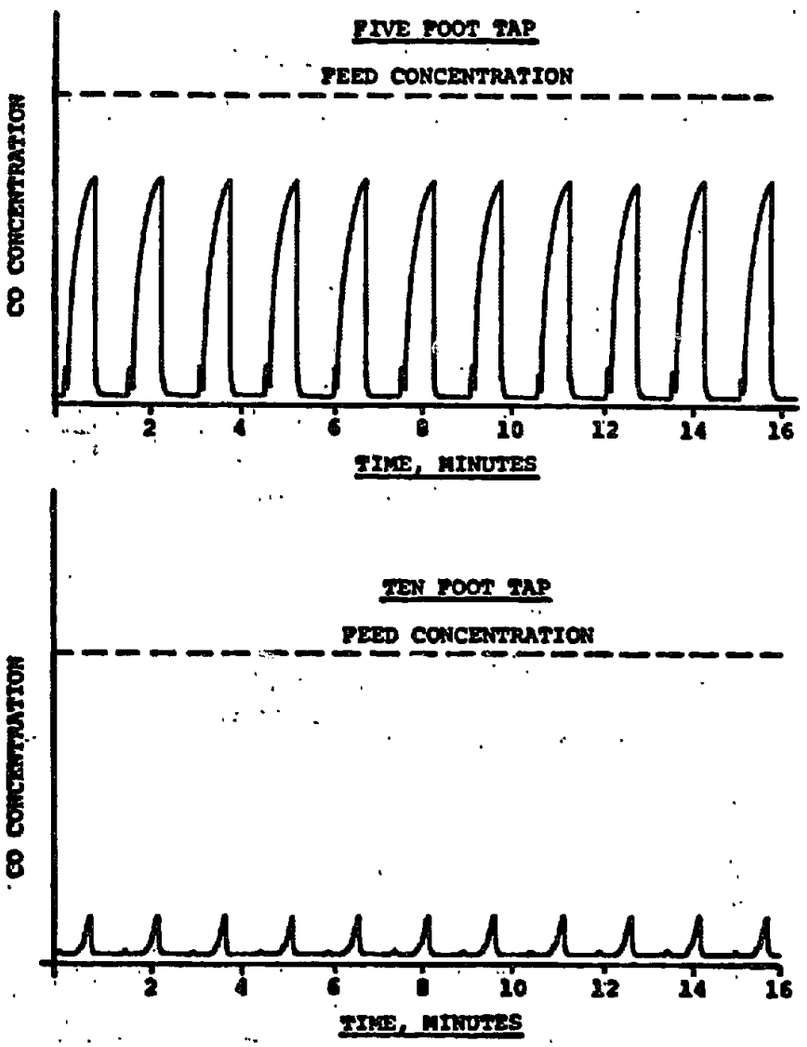

FIGURE 8

CO BREAKTHROUGH CURVES FOR 12 LITERS/MIN. OF 25% CO/75% N_2 DISPROPORTIONATION FEED, A 1½ MINUTE CYCLE TIME, A 270°C OVEN TEMPERATURE, A 5 PSIG EXIT PRESSURE, AND 1/8" EXTRUDATES OF CATALYST NO. AS-8209-14-2

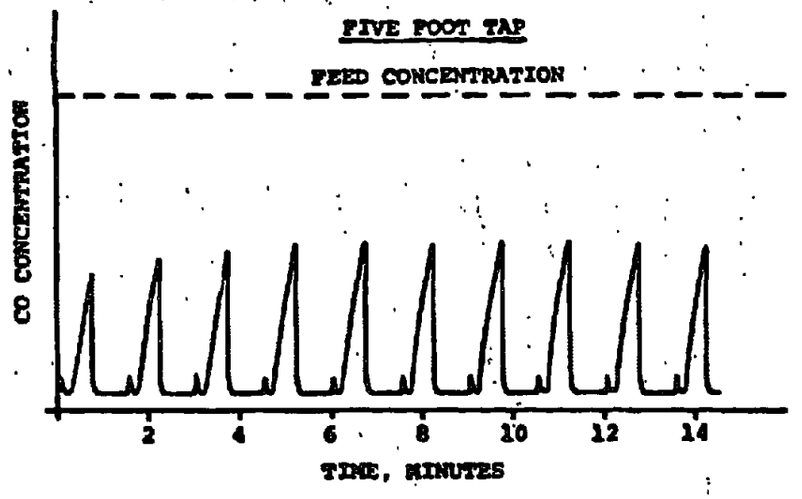

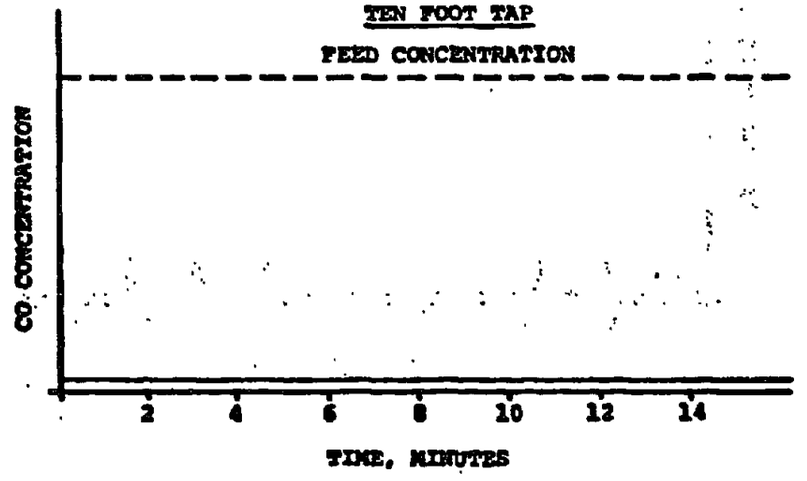

The reactors sized for the Chapter VII economic studies assumed a maximum seven foot long reaction zone for catalysts developed to date, and a maximum three and a half foot long reaction zone for a catalyst that could result from some future development effort.

Reaction zone lengths for the high pressure steaming step were considerably shorter than those found for the disproportionation step. They are discussed further in subsequent sections on steam utilization and ancillary reactions.

METHANE PRODUCTION RATES

The methane production rates, defined as the amount of methane produced during the steaming step divided by the grams of catalyst present in the equilibrium zone, and obtained with the mini PDU reactor, were consistently in good agreement with the 2-5 ml CH_4/gm-cycle rates obtained with the catalyst screening unit during the Chapter V catalyst development studies.

CO UTILIZATIONS

Table II shows the CO utilizations, defined as the amount of produced methane divided by the amount of reacted CO, were 19-20% (19) for a typical set of runs made with the mini PDU reactor. These values were in good agreement with the 18-20% efficiencies observed with the catalyst screening unit during the catalyst development studies. Table II also shows that the carbon balances around the reactor over the course of the cycles were ~94%, an indication of the experimental error.

TABLE II

MINI PDU CARBON BALANCE RUNS WITH CATALYST NO. AS-8209-14-22

CYCLE NO.	CARBON IN: LITERS OF CO ENTERING DURING DISP. STEP	CARBON OUT: LITERS OF CO LEAVING DURING DISP. STEP	+ LITERS OF CO_2 LEAVING DURING DISP. STEP	+ LITERS OF CO_2 LEAVING DURING STEAMING STEP	+ LITERS OF CH_4 LEAVING DURING STEAM-[2] STEP	= TOTAL LITERS OF CARBON SPECIES LEAVING	TOTAL CARBON OUT/TOTAL CARBON IN	CO UTILIZATION (CH_4 PRODUCED)(100)/(CO IN)[1]
8	5779	0	2103	2246	1090	5439	0.94	20.0%
11	5779	0						
15	5779	0	2155	2225	1074	5454	0.94	19.7%
19	5779							
23	5779	0	2165	2230	1098	5493	0.95	20.0%
25	5779							
29	5779	0	2123	2200	1075	5398	0.93	19.9%
31	5779							

[1] Normalized to equal the total number of liters of carbon-containing compounds leaving the reactor.

[2] Also includes a small amount of CH_4 present in the disproportionation effluent.

The descrepancy between the theoretical 25% efficiency and the measured 18-20% efficiencies could be attributed to analytical error and to some, as yet undefined side reaction (19). One such side reaction might be the reaction of water adsorbed on the nickel catalyst, left over from the steaming step, with the CO in the disproportionation feed gas to form hydrogen via the water gas shift reaction.

STEAM UTILIZATIONS

The steam utilization is defined as the amount of steam used in the steaming reaction divided by the amount of steam fed into the reactor. The amount of steam used for the reaction was calculated from the amount of methane produced during the steaming step. The amount of steam fed into the reactor was found from noting how much steam was pumped into the reactor up to the elution of the relatively sharp steam front, the point at which the steaming step for a commercial reactor would be terminated.

Table III shows that of all the steam pumped into the reactor up until the breakthrough of the steam front, 11.3% of it ((1.7)(100)/(15.0) = 11.3) was used for the COthane reaction, 10.0% ((1.5)(100)/(15) = 10.0) of it filled the void spaces in the reactor, and 78.7% ((11.8)(100)/(15.0) = 78.7) of it was evidently adsorbed onto the catalyst. Since there were approximately 550 grams of reduced catalyst in the reactor, the adsorbed water loading amounted to 2.1 wt.% ((11.8)(100)/(550) = 2.1), a value that is reasonable, in view of the alumina content of the catalyst, for the 0.14 P/P_o ratio (where P = the partial pressure

TABLE III

STEAM BALANCE FOR THE STEAMING STEP UP TO THE ELUTION OF THE STEAM FRONT

1.	TOTAL STEAM IN:		15.0 GRAMS
2.	TOTAL STEAM OUT:		
	USED IN COTHANE REACTION	1.7 GRAMS	
	ESTIMATED VOID SPACES	1.5 GRAMS	
	ESTIMATED ADSORBED (15.0-1.7-1.5)	11.8 GRAMS	
			15.0 GRAMS

of the steam, and P_o = the vapor pressure of the steam) used for the steaming step.

This adsorbed steam is not used, and is presumably desorbed during the ensuing depressurization and flushing steps. Since the loss of an amount of steam that is 7 times the stoichiometric amount of steam required for the COthane reaction (11.8/1.7 = 6.9) will increase the methane production cost by ~$2/MM BTU (1), final commercialization of the COthane process will require the development of a more hydrophobic catalyst, probably one with a different binder.

ANCILLARY REACTIONS

A. Reaction of the Nickel Catalyst With Steam

It was noted during many of the mini PDU runs that a significant amount of hydrogen was present in the product gas whenever a large amount of excess steam was used in the steaming step (20). It is believed that this hydrogen is formed from the reaction of steam with the nickel in the catalyst according to the reaction, $Ni + HOH \rightleftharpoons NiO + H_2$. It is further believed that this nickel oxide is then reduced with some of the CO introduced during the disproportionation step, according to the reaction, $NiO + CO \rightleftharpoons Ni + CO_2$. Consequently, there is a zone in the catalyst bed, presumably located near the inlet end of the reactor, which is oxidized, and then reduced, during each process cycle.

The hydrogen produced this way during the steaming step could be troublesome if it were eluted simultaneously from the bed with the product methane. However, prior runs on the catalyst screening unit (18) indicated that the hydrogen does not leave the bed until after the CH_4/CO_2 front has passed, presumably because the hydrogen formed upstream of that front reacts with the active carbon in that front to form methane.

In order to verify these past observations, spot samples were taken from the mini PDU reactor during the steaming step and were analyzed for their hydrogen content. Figure 9 shows that the amount of hydrogen relative to the amount methane was indeed low prior to the arrival of the steam front, and that hydrogen was a significant component of only the small amount of non-condensible gas that eluted from the bed during the steaming step.

As stated previously, the hydrogen is formed from the reaction of the steam with the nickel in the catalyst, via $Ni + HOH \rightleftharpoons NiO + H_2$. The value of P_{H_2}/P_{H_2O}, calculated from the amount of collected hydrogen and the amount of steam that passed through the bed after the passage of the steam front, was found to be 0.036, a value that was in general agreement with the 0.007 (for solid nickel) - 0.09 (for active nickel) range given in the literature (29).

FIGURE 9

HYDROGEN CONTENT OF NON-CONDENSIBLE SAMPLES OF THE STEAMING STEP EFFLUENT

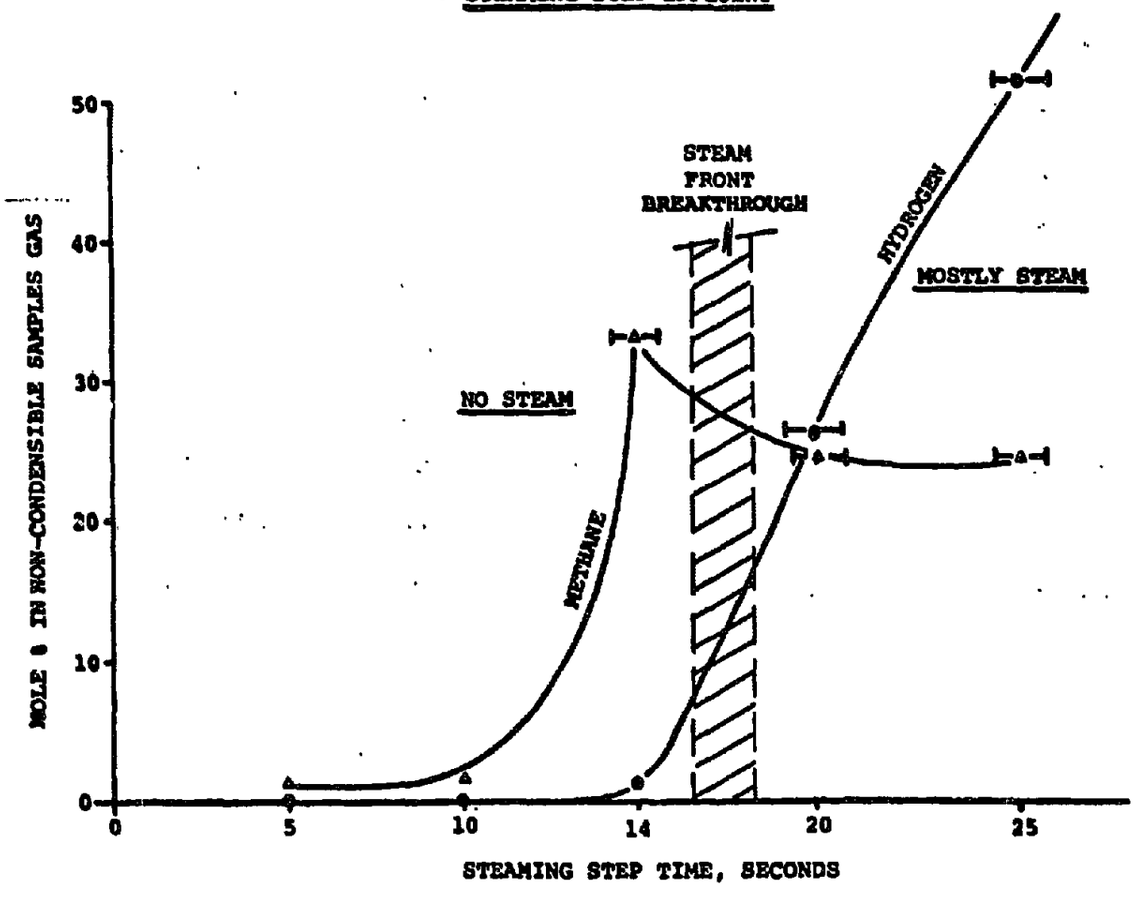

B. CO Chemi-sorption

The typical mini PDU results given in Table II indicate that the CO_2/CH_4 molar ratio in the steaming/depressurization/flush effluent was more than twice the equimolar value expected from equation, $2C^* + 2\ H_2O \rightleftharpoons CH_4 + CO_2$. Furthermore, the amount of CO_2 collected in the disproportionation step effluent was less than the sum of the amounts of CO_2 and CH_4 collected in the steaming/depressurization/flush effluent, as predicted by the COthane equations, $4CO \rightleftharpoons 2C^* + 2CO_2$ and $2C^* + 2H_2O \rightleftharpoons CH_4 + CO_2$. Both of these phenomena are probably caused by the chemi-sorption of CO (30) on the nickel catalyst at the moderate <300°C disproportionation temperatures present in the bed during these cycles. The chemi-sorbed CO reacts with the steam via the reaction $4CO + 2H_2O \rightleftharpoons CH_4 + 3CO_2$ (the overall COthane reaction), and thus produces relatively more CO_2 per mole of methane than that which results from the second step COthane reaction, $2C^* + 2H_2O \rightleftharpoons CH_4 + CO_2$ (19).

IV MINI PDU RUNS WITH REACTIVE DILUENTS

Many CO-containing waste gas streams, which are potential feed streams for the COthane process, also contain varying amounts of hydrogen, water, or oxygen. All of these components might be expected to react with any active carbon that is formed from the disproportionation of the CO and thus lessen the CO utilization, which is defined as the amount of methane produced during the steaming step divided by the total amount of CO reacted.

The expectation of lower CO utilization is justified when the thermodynamic equilibrium for such mixtures are calculated at the COthane process conditions. Table IV shows(19) that for a feed gas containing 0.25 gram moles of CO, 0.05 gram moles of H_2O, and 0.7 gram moles of N_2, only 0.085 gram moles of active carbon, C*, can be expected to form, versus the ~0.125 gram moles of C* that would be expected to form if there were no water present. This means that in order to "load" the catalyst bed up to its full potential with C*, more feed gas would be required to supply more CO, which in turn would lower the CO utilization.

Table V shows (19) that the same behavior could be expected for feed streams containing 6 and 10 mole % H_2. Furthermore, Table VI shows(19) that if both hydrogen and water are present in relatively large amounts, as would be the case for untreated, cooled carbon black off-gas, no C* would be expected to form at all. In fact that mixture is shown to be a net C* consumer,

TABLE IV

EQUILIBRIUM PRODUCT DISTRIBUTION FOR DISPROPORTIONATION

FEED GAS CONTAINING WATER

	Feed	Δ Moles	Equilibrium, moles	Equilibrium mole fr.
CO	0.25	-.24929616	.00070384	.00080319
H_2	0.0	+.00191024	.00191024	.00217988
H_2O	0.05	-.04045933	.00954067	.01088736
N_2	0.70		.70	.79880677
C*		+.08514387	.08514387	
CO_2		+.14487775	.14487775	.16532761
CH_4		+.01927455	.01927455	.02199520
Sum excluding C*			.87630705	

TABLE V

EQUILIBRIUM PRODUCT DISTRIBUTION FOR DISPROPORTIONATION

FEED GAS CONTAINING HYDROGEN

CASE I

	Feed	Δ Moles	Equilibrium, moles	Equilibrium mole fr.
CO	0.25	-.249372	.00062835	.00074349
H_2	0.0625	-.060354	.00214572	.00253890
H_2O	0.0	+.0099213	.00992129	.01173927
N_2	0.6875		.6875	.81347755
C*		+.104430	.10442998	
CO_2		+.119725	.11972518	.14166363
CH_4		+.0252165	.02521649	.02983716
Sums excluding C*			.84513703	
Sums including C*			.94956701	

CASE II

	Feed	Δ Moles	Equilibrium, moles	Equilibrium mole fr.
CO	0.25	-.24938224	.00061776	.00074728
H_2	0.10	-.09725324	.00274676	.00332263
H_2O	0.0	+.01276510	.01276510	.01544136
N_2	0.65		.65	.78627549
C*		+.08882960	.08882960	
CO_2		+.11830857	.11830857	.14311251
CH_4		+.04224407	.04224407	.05110073
Sums excluding C*			.82668226	
Sums including C*			.91551186	

TABLE VI

EQUILIBRIUM PRODUCT DISTRIBUTION FOR DISPROPORTIONATION FEED GAS CONTAINING HYDROGEN AND WATER (SIMILAR TO COOLED CARBON BLACK TAIL GAS)

	Feed	Δ Moles	Equilibrium, moles	Mole Fraction
CO	0.15	-.149448	.00055176	.000647371
H_2	0.15	-.145934	.00406595	.004770513
H_2O	0.05	-.033631	.01636940	.019205949
N_2	0.65		.65	.76263434
C*	Present	-.0318735	-.03187350	
CO_2		.0915394	.09153942	.10740170
CH_4		.0897823	.08978232	.10534012
Sum excluding C*			.85230885	

indicating the COthane process could not operate with untreated carbon black off-gas.

Similarly, the presence of oxygen in the feed gas can be expected to reduce the CO efficiency by its propensity to oxidize either the CO or the C*. However, if the oxygen level is relatively low, both the lowered CO utilization and the higher exothermicity might still be acceptable.

These equilibrium-based assumptions were checked with a series of mini PDU runs using unregenerated catalyst AS-8209-14-22, a 1½ minute cycle, a 24 liter/minute feed flowrate, and various hydrogen, water, and oxygen-containing feed streams(19,20). In most cases the runs were made with an accompanying blank run, which used a feed stream that contained the same amount of CO, but none of the other reactive components. In such cases the oven temperature was adjusted so that the maximum tube temperatures for the two comparison runs were the same.

Table VII shows that the CO utilization for a feed stream containing 5-10% mole % H_2O was only slightly effected by the water. The ~3% decrease in CO utilization was far less than the expected ~32% decrease ((0.125-0.085)/(0.125)=0.32) predicted by the equilibrium calculations presented in Table IV. Similarly, Table VIII shows that the CO utilization for a feed stream containing 5-10% hydrogen actually increased by 26-41%, instead of decreasing by 17-29% as predicted by the equilibrium calculations presented in Table V. Finally, Table IX shows

TABLE VII

EFFECT OF WATER ON THE METHANE EFFICIENCY WITH THE MINI PDU REACTOR

CATALYST NO. AS-8209-14-22

FEED GAS COMPOSITION	FEED GAS FLOWRATE L/MIN	MAXIMUM DISP. TEMP., °C	(1) CO_2 IN DISP. EFFLUENT, ML	(2) CH_4 IN DISP. EFFLUENT, ML	(3) CO_2 IN STEAM EFFLUENT, ML	(4) CH_4 IN STEAM EFFLUENT, ML	CO UTILIZATION $\frac{(4)\ (100)}{(1)+(2)+(3)+(4)}$
25% CO 75% N_2	24	~300	1350	10	1350	620	18.6
25% CO 5% H_2O 70% N_2	24	~300	1450	15	1325	620	18.2
25% CO 75% N_2	24	~300	1350	15	1325	620	18.7
25% CO 10% H_2O 65% N_2	24	~300	1460	20	1300	620	18.2

TABLE VIII

EFFECT OF HYDROGEN ON THE METHANE EFFICIENCY WITH THE MINI PDU REACTOR

CATALYST NO. AS-8209-14-22

FEED GAS COMPOSITION	FEED GAS FLOWRATE L/MIN	MAXIMUM DISP. TEMP., °C	(1) CO_2 IN DISP. EFFLUENT, ML	(2) CH_4 IN DISP. EFFLUENT, ML	(3) CO_2 IN STEAM EFFLUENT, ML	(4) CH_4 IN STEAM EFFLUENT, ML	CO UTILIZATION $\frac{(4)\ (100)}{(1)+(2)+(3)+(4)}$
25% CO 75% N_2	24	~300	1200	45	1100	600	20.4
25% CO 5% H_2 70% N_2	24	~300	1000	60	1250	800	25.7
25% CO 75% N_2	24	~300	1200	10	1300	580	18.8
25% CO 10% H_2 65% N_2	24	~300	800	70	1350	800	26.5

TABLE IX

DETERMINATION OF THE CO EFFICIENCY WITH SIMULATED COOLED CARBON BLACK TAIL GAS

CATALYST NO. AS-8209-14-22

FEED GAS COMPOSITION	FEED GAS FLOWRATE L/MIN	MAXIMUM DISP. TEMP., °C	(1) CO_2 IN DISP. EFFLUENT, ML	(2) CH_4 IN DISP. EFFLUENT, ML	(3) CO_2 IN STEAM EFFLUENT, ML	(4) CH_4 IN STEAM EFFLUENT, ML	CO UTILIZATION $\frac{(4)\ (100)}{(1)+(2)+(3)+(4)}$
15% CO 15% H_2 5% H_2O 65% N_2	24	~305	450	130	1125	600	26.0
15% CO 15% H_2 5% H_2O 65% N_2	24	~337	250	520	850	600	27.0

that the ~26% CO utilization for a simulated carbon black off-gas feed stream was well above the ~20% utilization for hydrogen and water-free streams, as well as the zero utilization predicted by the equilibrium calculations presented in Table VI.

This data indicates that at the low pressure of the disproportionation step, equilibrium is not reached during the short time that is required for the feed gas to pass through the reactor. It is likely that during this short residence time an initial, fast reaction predominates, such as CO + $H_2 \longrightarrow C^* + H_2O$, which would permit one gram mole of C* to form from one gram mole of CO, instead of from two gram moles of CO, as is required by the disproportionation reaction. This lower CO consumption, in turn, would result in a higher CO utilization. Such increased performance is particularly pertinent to the handling of cooled carbon black off-gas, since there will be no technical need to remove the hydrogen prior to sending it to the COthane unit.

It is also apparent that the reactions involving water, particularly $2C^* + 2H_2O \rightleftharpoons CH_4 + CO_2$, are relatively slow at the low pressure of the disproportionation step. This means that a feed gas with a relatively high CO concentration and a ~100°F dew point could be sent to the COthane unit without being dried.

V CATALYST DEVELOPMENT

The development of a more effective COthane catalyst has entailed the construction of a suitable catalyst screening unit, and the subsequent testing of different catalyst formulations in that screening unit.

CATALYST SCREENING UNIT

Figure 10 shows the flow diagram for the catalyst screening unit. During the four minute disproportionation step 1 liter/minute of a 20 vol.% CO/80 vol.% N_2 gas mixture is fed from a cylinder, through a preheat coil, through the reactor, and on through a back pressure regulator set at 5 psig. The effluent gas is either vented or collected in a gas collection vessel. The preheat coil and reactor are immersed in a fluidized bed temperature bath, which is usually maintained at 270°C. Upon completion of the disproportionation step, the system is pressurized to 150 psig with nitrogen, and the four minute steaming step is begun. A little over 0.2 ml/min of distilled water is pumped through the preheat coil, where it is vaporized, and on through the reactor. The product methane and carbon dioxide are displaced through a back pressure regulator set at 150 psig, and into either the vent line or a second gas collection vessel. The system is then slowly depressurized to ~1 psig over a one minute period, and the released gas is again either vented or collected in the same gas collection vessel used for the steaming step.

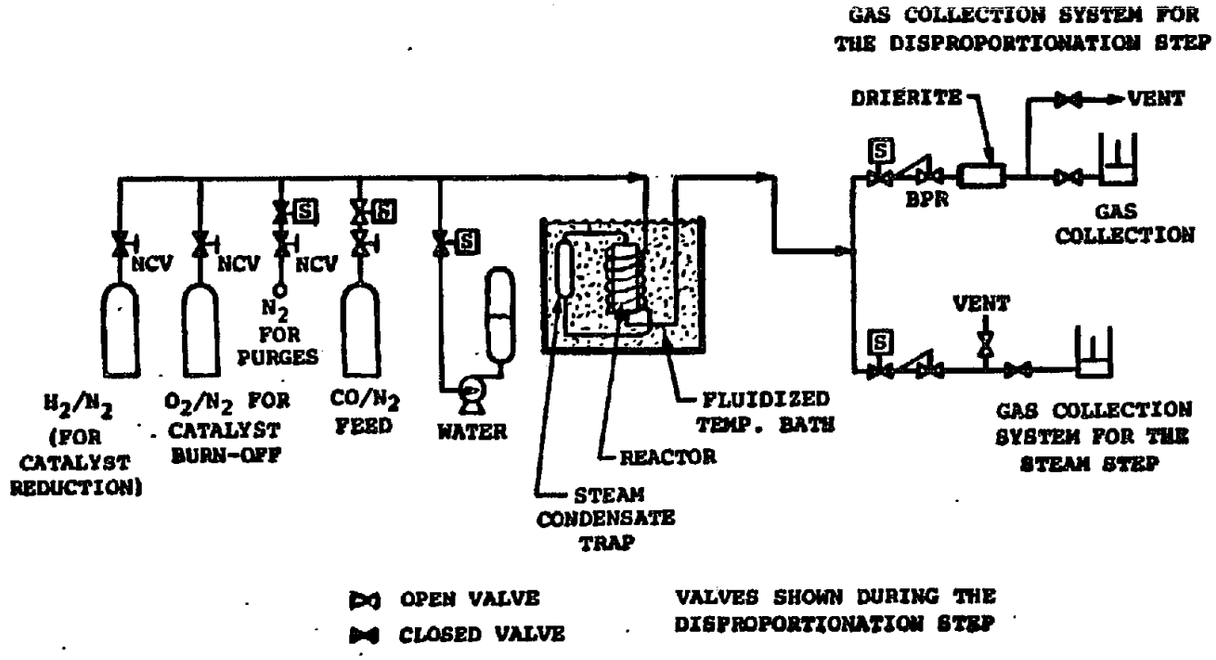

FIGURE 10

FLOW DIAGRAM FOR THE CATALYST TESTING UNIT

The unit repeats this nine minute cycle automatically. During most of the cycles the effluent streams are vented. However, during other, designated cycles the gas samples are collected for the disproportionation and steaming/depressurization steps, and are analyzed for their methane and carbon dioxide contents. The quantities of these gases indicate the performance of the catalyst during each step of the COthane cycle. The most important measure of the performance of a catalyst is its methane production rate, expressed as ml of methane/gm of catalyst-cycle.

The 0.033 gm moles {(4)(0.2)(1)/(24.2) = 0.033} of carbon monoxide fed into the reactor would require, from Equation 3, 0.017 gm moles {(0.5)(0.033) = 0.017} of water, if all of the carbon monoxide should disproportionate. The actual amount of water fed to the reactor was 0.044 gm moles {(4)(0.2)/(18)= 0.044}, or 2.1 times {0.044/0.017 = 2.1} greater than would be theoretically required. Furthermore, the 0.8 liters {(4)(0.2)(1)= 0.8} of CO fed to the eight grams of catalyst in the reactor is capable of theoretically yielding 25 ml of methane/gm of catalyst {(0.25)(0.8)(1000)/(8) = 25} during each complete COthane cycle. Since this amount of methane is considerably greater than the 5 to 10 ml/gm-cycle of methane that was actually produced by most of the tested catalysts during each cycle, it can be concluded that these measured rates were not limited by the amount of CO and water fed to the reactor during each cycle.

Figure 11 shows that the catalyst screening reactor itself consisted of a 5" long, 5/8" O.D. piece of stainless steel tubing with a 20 cm^3 capacity that held the 8 gm catalyst sample and ~10 grams of diluent quartz chips. A thermocouple, placed approximately one third the distance down from the top of bed, served as the standard temperature indicator for all of the test runs. In each case the temperature at that point would be close to the temperature of the fluidized temperature bath (typically 270°C) at the beginning of the disproportionation step. That bed temperature would then climb during the disproportionation step, level out (typically ~300°C) during the steaming step, and return back down to the fluidized bath temperature by the end of the depressurization step. During the initial runs made with this reactor, a second thermocouple was placed in the space directly above the bed, in order to verify that the 20 feet of 1/8" preheat tubing was sufficiently long to bring the temperatures of both the disproportionation and steaming influents up to the fluidized bath temperature.

The 270°C to 300°C temperature swing experienced by the catalyst bed during each cycle is representative of what the catalyst bed in the presently envisioned commercial reactor would experience under analogous process conditions. Consequently, this catalyst screening unit is considered to be an appropriate tool to test improved catalyst formulations.

Each of these new formulations were placed in the catalyst screening reactor, heated with the fluidized temperature bath to 400°C, reduced with a 4 vol.% H_2/96 vol.% N_2 stream, cooled to 270°C, and then subjected to the first set of test cycles.

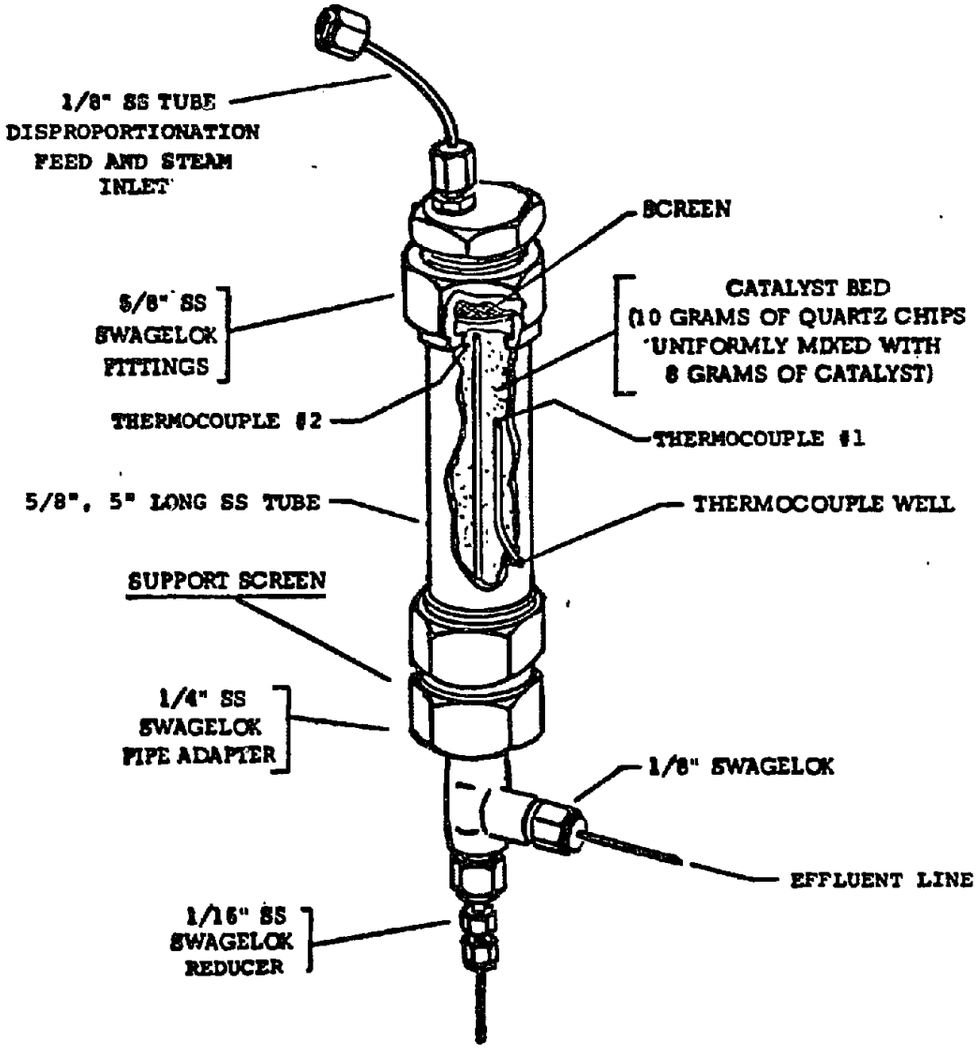

FIGURE 11

STAINLESS STEEL PACKED BED REACTOR

After this first set of cycles the catalyst was usually reheated to 400°C, burnt off with a 1 vol.% O_2, 99 vol.% N_2 stream, reduced with a 4 vol.% H_2/96 vol.% N_2 stream, cooled down, and subjected to the second set of test cycles.

CATALYST DEVELOPMENT - FORMULATION STUDIES

The catalyst used in the COthane process has to catalyze both the disproportionation of CO to active surface carbon and CO_2, and the reaction of the active surface carbon with steam to form equimolar quantities of methane and carbon dioxide. In order to perform these tasks satisfactorily, the COthane catalyst must: a) have a high capacity and selectivity for the formation of active carbon over a long period of time, b) either have a negligible tendency to form inactive carbon, or if inactive carbon is formed, be able to withstand oxidative regenerations, and c) have good mechanical stability. Furthermore, the calculations described in Appendix I show that a nickel surface area of ~32 m^2 Ni/gm of catalyst is needed for a theoretical 1 wt.% loading of active surface carbon. Since all supported nickel catalysts are prone to sintering and forming larger nickel particle sizes (15-20 nm) with an attendant lessening of the nickel surface area at elevated (>200°C) temperatures, the attainment of a 32 m^2 Ni/gm surface area can only be realized with high concentrations of nickel (60-70%) in the catalyst.

These characteristics were partially met by the nickel-zirconia catalyst originally developed for the COthane process. This formulation was prepared by the addition of 1 liter of 1.15 molar solution of sodium hydroxide to a 1 liter solution containing 0.5 mole (145.5 gms) of $Ni(NO_3)\cdot 6H_2O$ and 0.0375 mole (10.0 gms) of $ZrO(NO_3)_2\cdot 2H_2O$. The resulting gel was then filtered, washed with distilled water, and subsequently dried at 65°C in air. The resulting catalyst was reduced in a stream of 5% hydrogen in nitrogen with the temperature programmed to increase gradually to 400°C, where it was maintained for several hours.

Efforts to improve the long term capacity, selectivity, and activity of this original formulation during the initial stage of the catalyst development program were directed towards trying new matrixing agents, new metal compositions, and different synthesis techniques. Furthermore, the attainment of good mechanical stability resulted from the continual product development effort which accompanied the large scale production of five-pound batches of the more promising catalyst formulations required for the mini PDU unit, as dictated by the mini PDU studies.

Twenty-four catalysts were tested during this first stage of the catalyst development effort. The results obtained in this period indicated that the catalysts fell into three classifications. Tables X through XV lists the characteristics, ingredients used during synthesis, and analyses for all of the

TABLE X

CHARACTERISTICS OF TYPE I CATALYSTS

CAT. NUMBER	RUN NUMBER	USED CAT. NO.	REPORT REF. #	H_2 RED.	SECOND RUN 2nd CYCLE CH_4 ML/GM.	SECOND RUN FINAL CYCLE() CH_4 ML/GM.	CARBON WT. %	CATALYST SURFACE AREA FRESH	CATALYST SURFACE AREA USED	Ni CRYSTALLITE SIZE CHANGE NM FRESH	Ni CRYSTALLITE SIZE CHANGE NM USED	% Ni REDUCED	FRESH CATALYST H/Ni
AS-5005-69-13	EL-5342-59	AR-5404-46	11, 12,	525°C	~17.5(4)	5.5(130)	4.5	87	63	10.0	13	80%	0.037
AR-5404-37-18	EL-5342-39	AR-5404-38	11, 12,	500°C	14.5	5.1(175)	4.7	122	74	11.9	14.0		0.027
AR-4988-96-32	EL-5342-24	AR-5404-34	10,	600°C	13	4.8(190)	3.7	135		8.5	9.5		0.041
AS-5005-71-8	MW-8175-5	AR-5404-51	12,	516°C	~10.0(10)	4.0(160)	8.0	78	75	10.2		80%	0.044
LE-4441-36A	LE-3353-27	AS-5005-51	8, 9, 10,	400°C IR[a]	11	---	1.2	144	60	6.3	20.0	40%/80%	0.058
AS-5005-38-28	EL-5342-29	AR-5404-35	10,	400°C IR	8.8	3.8(45)	2.2	53		14.8			
AS-5005-75-18	MW-8175-6	AR-5404-52	12,	523°C	8.8	4.3(200)	8.1	135	115				0.048
AS-5005-3-25	MW-8175-7	AR-5404-56-13	13, 14, 17	400°C IR	12.5	3.0(500)	16	193	135		12.9	76%[c]	0.071
AS-5005-86-17	MW-8175-9	AR-5404-56-26	13, 14, 17	400°C IR	.10	4.1(200)	2.0	61	38				
AS-5005-50-17	MW-8175-10	AR-5404-56	13, 14, 17	400°C IR	L.T.T.[b] (220°C)	2.4(300)	6.0	101	64			75%[c]	0.037

a) In Reactor (IR).

b) Low temperature test (November report).

c) Used catalyst result.

TABLE XI

INGREDIENTS AND ANALYSES OF TYPE I CATALYSTS

CAT. NUMBER	BASIC SYNTHESIS TECHNIQUE[b]	COMPONENTS USED IN THE SYNTHESIS	CHEMICAL COMPOSITION				
			% NiO	% Al_2O_3	% ZrO_2	% Other	% LOI
AS-5005-69-13	B	$Ni(NO_3)_2$ and $ZrO(NO_3)_2$; $Pd(NO_3)_2$ added to calcined extrudate	66.9	15.6	8.4	2.3 PdO	5.6
AR-5404-37-18	A	$Ni(NO_3)_2$ and $Al(NO_3)_3$	72.5	17.5			7.2
AR-4988-96-32	B	$Ni(NO_3)_2$ and $Al(NO_3)_3$	66.2	24.6			6.4
AS-5005-71-8	B	$Ni(NO_3)_2$ and $ZrO(NO_3)_2$	70.0	15.0	8.0		7.0
LE-4441-36A	C	$Ni(NO_3)_2$ and $ZrO(NO_3)_2$	68.0	17.0	10.0		5.0
AS-5005-38-28	B	$Ni(NO_3)_2$ and TiO_2 powder (as a slurry)	78.2	6.1		11.0(TiO_2)	3.0
AS-5005-75-18	B[a]	$Ni(NO_3)_2$, $Al(NO_3)_3$ and Ca $(NO_3)_2$	58.7	23.6		4.4(CaO)	12.0
AS-5005-3-25	A	$Ni(NO_3)_2$ and $ZrO(NO_3)_2$	54.3	15.6	19.1		9.8
AS-5005-86-17		Commercial Raney Nickel leached with NaOH	64.7	4.3			
AS-5005-50-17	B	$Ni(NO_3)_2$ and $ZrO(NO_3)_2$	73.5	15.2	17.4		3.9

a) Na_2CO_3 was used as the precipitating base.

b) See Appendix II.

TABLE XII

CHARACTERISTICS OF TYPE II CATALYSTS

CAT. NUMBER	RUN NUMBER	USED CAT. NO.	REPORT REF. NO.	H_2 RED.	SECOND RUN 2nd CYCLE CH_4 ML/GM.	SECOND RUN FINAL CYCLE() CH_4 ML/GM.	CARBON WT. %	CATALYST SURFACE AREA FRESH	CATALYST SURFACE AREA USED	Ni CRYSTALLITE SIZE CHANGE NM FRESH	Ni CRYSTALLITE SIZE CHANGE NM USED	% Ni REDUCED	FRESH CATALYST H/Ni
AS-5005-31-15	EL-5342-21	AR-5404-33	10,	---	7.6	4.5(42)	0.4						
AR-4988-87-27	EL-5342-13	AR-5404-32	10,	600°C	5.5	4.3(25)	0.18	167		12.5	15.3	40-50%	0.069
AS-5005-53-10	EL-5342-35	AR-5404-39	10,	600°C	5.6	4.0(175)	0.20	135	92	5.6	9.8	40%	0.067
AS-5005-67-12	EL-5342-55	AR-5404-45	11, 12	525°C	4.5	3.7(25)	0.60			23.7			
AS-5005-66-11	EL-5342-51	AR-5404-44	11, 12	550°C	4.4	5.0(200) (290°C)	2.1	62		16.0		70%	
AS-5005-70-10	EL-5342-61	AR-5404-47	12,	510°C	5.1	3.8(14)		135	76	13.0			0.052
AS-5005-72-11	MM-8175-1	AR-5404-50	12,	517°C	7.0	4.2(14)		73					0.029
AS-5005-53-10	MM-8175-8	AR-5404-56	13, 14, 17	580°C	5.7	3.5(500)	1.1	135	(118)				0.057[c]
AS-5005-87-14	MM-8175-11	AR-5404-57	14, 17, 18	620°C	H.T.T.[a] (341°C)	2.5(500)	~50			8.2		82%	0.056
AS-8209-2-32	MM-8175-12	AR-5404-58	14, 17, 18	629°C	4-H.O.T.[b]	2.8(850)		147	113	9.1	11.0	~78%	0.046/0.053[c]

a) High temperature test (15).

b) Catalyst regenerated four times via O_2 burn off.

c) Used catalyst result.

TABLE XII
(continued)

CHARACTERISTICS OF TYPE II CATALYSTS

CAT. NO.	RUN NO.	USED CAT. NO.	REPORT REF. NO.	H_2 RED.	FIRST RUN 2nd CYCLE CH_4 ML/GM.	FIRST RUN FINAL CYCLE() CH_4 ML/GM.	CARBON WT. %	CATALYST SURFACE AREA FRESH	CATALYST SURFACE AREA USED	Ni CRYSTALLITE SIZE CHANGE NM FRESH	Ni CRYSTALLITE SIZE CHANGE NM USED	% Ni REDUCED	FRESH CATALYST H/Ni
AS-5005-42-26	MW-8175-14	AR-5404-64-22	16,17,18,20	400°C IR	Special testing CO_2 and H_2 regeneration		N.D.	196	90		8.9	-84[c]	0.083/0.06[c]
AS-8209-6-13	MW-8175-15	AR-5404-65	16,17,18,20	400°C IR	5.0	4.3(400)	0.32	220	122		5.7		0.83
AS-8209-4-27	MW-8175-16	AR-5404-66	16,17,18,20	400°C IR	5.5	2.0(170)		136.			15.6	-85[c]	0.053
G-87	MW-8175-17	AR-5404-67	16,17,18,20	400°C IR	4.3	2.3(50)							
AS-8209-14-22	MW-8175-18	AR-5404-68-21	17,18,20,21	400°C IR	Special testing of O_2 regeneration (Type II)		0.2[d]	254	113	5.1	10.1	-84[c]	0.07/0.034[c]
AS-5005-61-19	MW-8175-19	AR-5404-70-9	18,19,20,21	400°C IR	Special testing of O_2 regeneration (Type I)		0.7[e]	132	70		13.0	-97[c]	0.03
AS-8209-6-13	MW-8175-22	AR-5404-71-9	18,19,20,21	400°C IR	4.2	3.5(1750)	0.5	220	76	4.9	7.2	-61[c]	0.83
AS-8209-18-30	MW-8175-23	AR-5404-72-5	19,20,21	400°C IR	7.4	2.8(900)	2.94	258	87		9.3	-75[c]	0.10
AS-8209-22-16	MW-8175-24	AR-5404-73-12	19,20,21	400°C IR	-4.0	3.0(350)	1.89	260	176				0.093
AS-8209-24-33	MW-8175-25	AR-5404-74-6	19,20,21	400°C IR		<2(6)	----						0.048
AS-8209-26-26	MW-8175-26	AR-5404-75	19,20,21	400°C IR	Special testing at 305°C -4.7	2.7(450)	----	240	48.7		13.0	100[c]	0.048
AS-5005-42-26	MW-8175-27	AR-5404-76-13	20,21	400°C IR	Special test using hydrogen instead of steam		----						
AS-8209-28-6	MW-8175-28	AR-5404-77-12	20,21	400°C IR	5.2	3.4(1200)	0.32		82.5		5.9	-34[c]	0.107
AS-8209-29-26	MW-8175-29	AR-5404-79-6	21	400°C IR	-6.5	2.8(450)	2.6	240					
AS-8209-31-18	MW-8175-30	AR-5404-80-5	21	400°C IR	6.0	2.9(1500)	0.59	238					0.071
AS-8209-32-23	MW-8175-31	None	22	400°C IR	5.5	2.9(4500)	26.45	230					0.096

c) Used catalyst result.

d) Carbon content after the last cycle of the month run.

e) Carbon content after last cycle of the twelth run.

TABLE XIII

INGREDIENTS AND ANALYSES OF TYPE II CATALYSTS

CAT. NO.	BASIC SYNTHESIS TECHNIQUE[a]	COMPONENTS USED IN THE SYNTHESIS	CHEMICAL COMPOSITIONS					
			% NiO	% SiO_2	% Al_2O_3	% ZrO_2	% Other	% LOI
AS-5005-31-15		Re-formulated commercial Nickel/Alumina catalyst						
AR-4988-87-27	B	$Ni(NO_3)_2$ and Cabosil (SiO_2) as a slurry	68.8	9.4	14.5			5.8
AS-5005-53-10	B	$Ni(NO_3)_2$ and Ludox AS-40 silica	70.0	9.8	11.2			7.9
AS-5005-67-12	C	$Ni(NO_3)_2$ and $ZrO(NO_3)_2$; KNO_3 added to calcined extrudates	70.3		11.3	8.5	1.5 K_2O	7.2
AS-5005-66-11	C	$Ni(NO_3)_2$, $Cu(NO_3)_2$ and $ZrO(NO_3)_2$	67.7		5.2	12.6	3.9 CuO	6.8
AS-5005-70-10	A	$Ni(NO_3)_2$, $Co(NO_3)_2$ and $ZrO(NO_3)_2$	37.2		15.0	9.2	29.5 CoO	8.9
AS-5005-72-11	B	$Ni(NO_3)_2$ and $Mg(NO_3)_2$	74.6		12.0		4.6 MgO	4.5
AS-5005-53-10	B	$Ni(NO_3)_2$ and Ludox AS-40 silica	70.0	9.8	11.2			7.9
AS-5005-87-14	B	$Ni(NO_3)_2$ and Ludox AS-40 silica	70.8	9.8	11.0			7.8
AS-8209-2-32	B	$Ni(NO_3)_2$ and Ludox AS-40 silica	70.3	10.2	11.2			7.7

a) See Appendix II.

TABLE XIII
(continued)

INGREDIENTS AND ANALYSES OF TYPE II CATALYSTS

CAT. NO.	BASIC SYNTHESIS TECHNIQUE	COMPONENTS USED IN THE SYNTHESIS	CHEMICAL COMPOSITIONS % NiO	SiO_2	Al_2O_3	LOI	Other	Other
AS-5005-42-26	B	$Ni(NO_3)_2$ and Ludox AS-40 Silica	70.0	9.8	11.2	7.9		
AS-8209-6-13	C[b]	$Ni(NO_3)_2$ and Ludox AS-40 Silica	68.5	24.5		5.4	0.33 Na_2O	
AS-8209-4-27	C	$Ni(NO_3)_2$ and Ludox AS-40 Silica	81.3	2.5	11.3	4.9		
G-87		Commercial Catalyst	~46					
AS-8209-14-22	C	$Ni(NO_3)_2$ and Ludox AS-40 Silica	69.2	12.1	12.7			
AS-5005-61-19	C[c]	$Ni(NO_3)_2$ and $Al_2(NO_3)$	72.5		17.4	7.2		
AS-8209-18-30	C	$Ni(NO_3)_2$, Ludox AS-40 silica and K_2CO_3.	70.2	7.8	10.8	7.5	1.4 K_2O	
AS-8209-22-16	C[b]	$Ni(NO_3)_2$, Ludox AS-40 silica and NaOH	53.3	37.4		8.6	0.33 Na_2O	
AS-8209-24-33	C[d,b]	$Ni(NO_3)_2$, Ludox AS-40 silica and $Ba(NO_3)_2$	60.7	31.8		3.6	3.1 BaO	
AS-8209-26-26	C[d,b]	$Ni(NO_3)_2$, Ludox AS-40 silica and $Li(NO_3)_2$	64.3	32.1		4.2	0.6 Li_2O	
AS-8209-28-6	C[b]	$Ni(NO_3)_2$, Ludox AS-40 silica and KOH	64.2	27.1		8.5	0.47 K_2O	
AS-8209-29-26	C[b]	$Ni(NO_3)_2$, Ludox AS-40 silica and $Fe(NO_3)_3$ and KOH	60.6	26.3		8.9	4.1 Fe_2O_3	~0.5 K_2O
AS-8209-31-18	C[b]	$Ni(NO_3)_2$, Ludox AS-40 silica and NaOH	64.6	26.0		9.1	0.62 Na_2O	
AS-8209-32-23	C[b]	$Ni(NO_3)_2$, Ludox AS-40 silica and $Ba(OH)_2$	64.8	24.9		9.6	1.2 BaO	

b) Extruded with a silica binder instead of alumina.

c) NH_4OH used instead of NaOH.

d) $(NH_4)2CO_3$ used as the precipitating agent inplace of NaOH

TABLE XIV

CHARACTERISTICS OF TYPE III CATALYSTS

CAT. NUMBER	RUN NUMBER	USED CAT. NO.	REPORT REP., NO.	H_2 RED.	SECOND RUN 2nd CYCLE CH_4 ML/GM.	SECOND RUN FINAL CYCLE CH_4 ML/GM.	CARBON WT. %	CATALYST SURFACE AREA FRESH	CATALYST SURFACE AREA USED	Ni CRYSTALLITE SIZE CHANGE NM FRESH	Ni CRYSTALLITE SIZE CHANGE NM USED	% Ni REDUCED
AS-5005-56-10	EL-5342-31	AR-5404-36	10	600°C	2.5	1.2(15)	0.7					
AS-5005-65-20	EL-5342-47	AR-5404-42	11, 12	800°C	<<1							
AS-5005-77	MM-8175-2	None	12	530°C	<1							
AS-5005-64-13	EL-5342-45	AR-5404-41	11, 12	800°C	3.5	2.9(33)		103	N.D.	14.7	N.D.	40-50%
AS-8209-1-5	MM-8175-13	AR-5404-60	14, 17, 18		<1	<1(30)		35				

TABLE XV

INGREDIENTS AND ANALYSES OF TYPE III CATALYSTS

CAT. NO.	BASIC SYNTHESIS TECHNIQUE[1]	COMPONENTS USED IN THE SYNTHESIS	CHEMICAL COMPOSITIONS					
			NiO	SiO_2	Al_2O_3	Other	Other	LOI
AS-5005-56-10	B	$Ni(NO_3)$, $Al(NO_3)_2$ and Ludox AS-40 SiO_2	59.6	8.3	22.6			11.2
AS-5005-64-13	A	$Ni(NO_3)_2$ and Cabosil SiO_2	~53	~12	~25			~10
AS-8209-1-5	-	Fe_4N, Fe_2N			10.4	68.2 Fe	5.5 N	

1) See Appendix II.

catalysts of each type. The methane production rate, expressed as ml of CH_4/gm of catalyst-cycle and listed in Tables X, XII and XIV for each catalyst after it had undergone a single burn-off, defines the catalyst type.

Type I catalysts showed high initial activity, often in excess of 10 ml CH_4/gm-cycle, in the first 5 cycles. The activity declined quickly through 20-25 cycles to 3-6 ml CH_4/gm cycle, at which point it appeared to stabilize. Type II catalysts had moderate initial activity of about 5-7 ml CH_4/ gm-cycle, which declined slowly and also stabilized to the 3-6 ml CH_4 range. Type III catalysts showed poor initial activity (less than 4 ml CH_4) and tended to reach a lower level. Figure 12 illustrates the performance of Type I and Type II catalysts.

The other data shown in Tables XI, XIII and XV, such as the carbon analysis on the used sample, X-ray analyses of fresh and used catalysts, surface area measurements, and H/Ni chemisorption ratios, characterize the important physical parameters of the catalyst. These results suggest that the residual, inactive carbon left on the catalyst after the steaming step tends to be higher for the catalysts having high initial activity and a Type I designation. It is speculated that the inactive carbon is formed during the initial cycles, when the CO conversions and attendant catalyst surface temperatures are unusually high. Type II catalysts do not have high initial exothermic activity, and consequently have substantially lower inactive residual carbon. Temperature control of the COthane

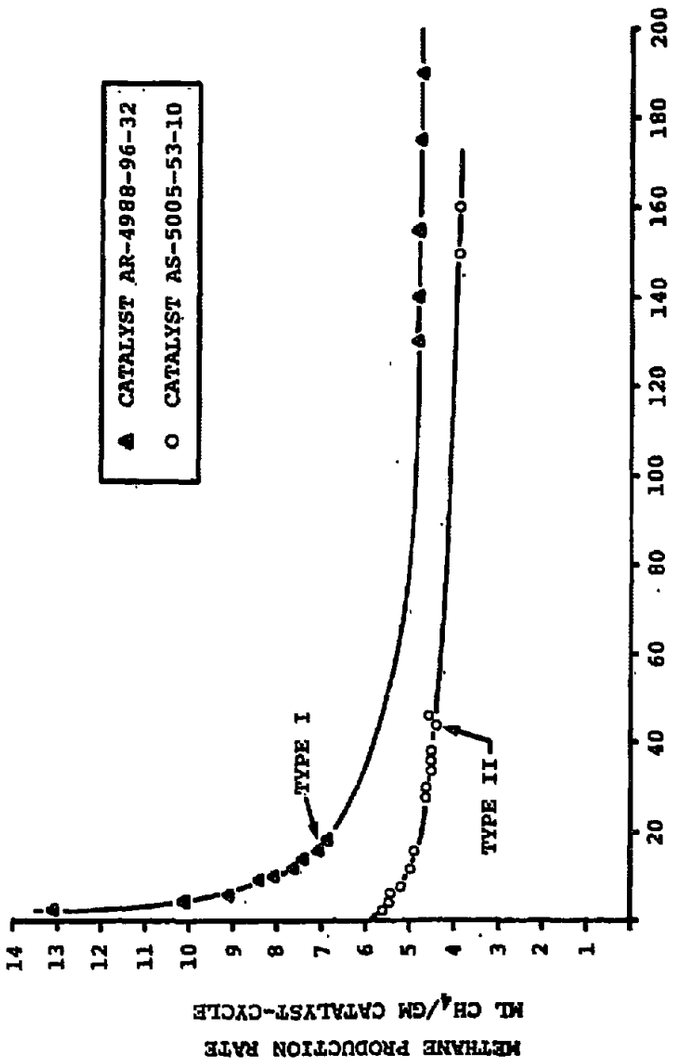

FIGURE 12

REPRESENTATIVE ACTIVITY FOR TYPE I AND TYPE II CATALYSTS

process using Type II catalysts is expected to be facilitated by their moderate initial activity.

Type I catalyst behavior was typically observed for alumina (AS-4988-96-32, AR-5404-37-18) and ziriconia (AS-5005-3-25, LE-4441-36A) based catalysts, although a Raney nickel catalyst (AS-5005-86-17) and a catalyst with a titania matrix (AS-5005-38-28) also showed Type I behavior. Type I performance was changed to Type II performance in zirconia-based catalysts with the addition of copper (AS-5005-66-11), cobalt (AS-5005-70-10), or potassium (AS-5005-67-12). The addition of 2.3% palladium to a zirconia catalyst (AS-5005-69-13) enhanced the type I performance and resulted in the highest initial activity observed in the COthane program.

Catalysts prepared with a silica matrix (AR-4988-87-27, AS-5005-53-10, AS-5005-2-32) showed Type II activity, produced the lowest level of inactive carbon, and maintained a stable 4-5 ml CH_4/gm-cycle production rate for over 200 cycles. A catalyst prepared with a magnesia matrix (AS-5005-72-11) also demonstrated Type II behavior.

In general the Type III catalysts listed in Tables XIV and XV were not reactive. Catalyst AS-8209-1-5 was an ineffective iron nitride composition. Catalyst AS-5005-64-13 was a silica matrix catalyst reduced at 800°C. The severity of the reduction generated a 14.7 nm nickel particle size and a 2.9 ml CH_4/gm-cycle methane production rate.

Several synthesis techniques were used in preparing the catalysts listed in Tables X through XV, and are detailed in Appendix II. The variability of these techniques did not cause meaningful differences in catalyst performance. Catalysts made with the rapid precipitation technique, the slow precipitation techniques, and different precipitating agents did not have significant differences in performance when they all contained the same nickel and matrix compounds.

The data for most of the Type I and Type II catalysts assembled in Tables X and XII was obtained from the second test run, after the initial test run and sequential oxidative regeneration had been completed. All the Type I and Type II catalysts show some degree of catalyst surface area loss after use. However, since Type I performance is exhibited both by fresh catalyst formulations with low surface areas (AS-5005-71-8, AS-5005-86-17, AS-5005-69-13) and by fresh catalyst formulations with high surface areas (AR-5404-37-18, AS-5005-3-25, AR-4989-96-32), it is concluded that the initial severe performance decline observed with all type I catalysts (Figure 12) is not caused by a rapid change in the catalyst surface area from a high value (~140 m^2/gm) to a low value (~70 m^2/gm). Additionally, since both Type I and Type II behavior is observed with high surface area catalysts and low surface area catalysts, it is concluded that the type of catalyst performance is independent of surface area.

Similarly, since catalysts with high nickel dispersions (AS-5005-3-25, LE-4441-36A, and AS-5005-75-18) and catalysts with lower nickel dispersions (AR-5404-37-18, AS-5005-50-17, and AS-5005-69-13) both showed Type I behavior, and since catalysts with high nickel dispersions (AR-4988-87-27, AS-5005-53-10, and AS-5005-70-10) also showed Type II behavior, the performance of the catalyst is not effected by the efficiency of the nickel dispersion.

Other parameters evaluated during the initial stage of catalyst development included the conditions of the air calcination and hydrogen reduction of fresh catalysts. The goals of these experiments was to maximize the percentage of the nickel in the reduced (metallic) state and minimize the formation of inactive nickel phases with the support, such as nickel aluminate and nickel silicalite.

Air calcination was necessary for the synthesis of a catalyst with good crush resistance, but was not critical for catalyst activity. Catalyst AS-5005-87-14 (12) did not undergo the usual 450-500°C air calcination, but was directly reduced at 630°C. The catalyst showed expected Type II performance. Various catalysts were air calcined at 450-500°C and subsequently reduced at different temperatures.

Although many fresh catalysts showed more efficient nickel reduction at higher temperatures, no important improvements in catalyst activity were apparent in the second run data for any of these catalysts. This result suggests that the active form of the operating catalyst is more strongly influenced by the process conditions (including the regeneration step) than the

activation conditions given the fresh catalyst. Furthermore, the silica-matrixed catalyst AS-5005-42-26, which underwent only the usual 400°C in-situ reduction, exhibited the same catalytic activity as did similar catalysts that had undergone high temperature pre-reduction steps (16).

Catalyst AS-5005-42-26 was also used to demonstrate the feasibility of using a CO_2/CO mixture to oxidize only the inactive carbon on the catalyst, and not the nickel catalyst itself (16). The results indicated that while the removal of the inactive carbon was satisfactory, there was still the same loss of activity between the CO_2/CO regenerations that were observed for the O_2 regenerations.

In another test, Type I catalyst AS-5005-50-17 (13) was evaluated at low (220°C) temperatures, in order to prolong the catalyst life through controlling the Type I exothermic activity and the attendant build-up of inactive carbon. Although the reactivity, and hence the magnitude of heat release, was controlled by starting the run at low temperatures, the long term performance declined rapidly, even as the reaction temperature was slowly increased to 285°C. Furthermore, the performance was not superior to the steady state performance of catalysts with silica matrices.

In a corollary experiment, a silica-matrixed Type II catalyst (12), AS-5005-87-14, was evaluated at a temperature which started out at the usual 270°C, and then was slowly increased to 341°C over 500 cycles. The catalyst had poor activity and a massive build-up of inactive carbon, indicating that the

operation of the COthane process with this catalyst is confined to a lower temperature regime.

In an attempt to increase the active carbon content of a Type II catalyst through increasing its nickel content, catalyst AS-8209-4-27 was prepared with substantially more nickel and less silica than the previous silica-matrixed catalysts. The test results showed that this high nickel, low silica catalyst had poor stability and a tendency to develop larger nickel particle sizes (16).

In summary, all of the data assembled in Tables X through XV suggest that three types of catalyst performance was observed for the COthane process. The performance produced by a particular catalyst appeared to be more strongly dependent on the chemical composition than on the physical properties. Although long term stability runs indicated that both Type I and Type II catalysts might have a 2-3 month service life (17, 18), the silica-matrixed Type II catalysts showed a more stable operation, moderate evolution of heat, and the lowest level of residual inactive carbon. These characterizations made the silica-matrixed Type II catalyst the most promising candidate for a further study into the effects of binder composition and dopant addition.

CATALYST DEVELOPMENT - BINDER/DOPANT STUDIES

The silica-matrixed catalyst AS-8209-6-13 was formulated with a sodium-doped silica binder by mixing the undoped nickel oxide/silica co-precipitate with a sodium hydroxide-gelled Ludox AS-40 silica. This catalyst, tested for ~400 cycles, showed a superior stability and a low residual level of inactive carbon, but an intolerance to repeated oxidative regenerations (16).

The increased fresh catalyst stability observed for AS-8209-6-13 may have resulted from the absence of acidic alumina in the formulation, or it may have resulted from the presence of sodium ions which came from the sodium hydroxide used during the bonding step. On the other hand, these sodium ions may have migrated to active sites during burn-offs, and thus may have caused the drop in activity that was observed after each burn-off, as indicated by the Electron Spectroscopy Chemical Analysis (ESCA) studies (22).

In an attempt to further increase stability by increasing the amount of the silica matrix, catalyst AS-8209-22-16 was formulated with a sodium-doped high silica, low nickel oxide co-precipitate and bonded with the same sodium-hydroxide-gelled silica procedure used for catalyst AS-8209-6-13. The test results showed no improvement in the activity, stability, or regenerability of this catalyst over the corresponding performance of catalyst AS-8209-6-13 (18).

In order to measure the effect of an increased sodium level, catalyst AS-8209-31-18 was formulated with the standard, soda-free nickel oxide-silica co-precipitate, and bonded with a

sodium hydroxide-gelled silica that contained twice as much sodium as was contained in the binder of catalyst AS-8209-6-13. The test results showed a slightly lower catalytic activity than that of catalyst AS-8209-6-13 (21).

In order to determine the effect of a different alkali metal dopant with an alumina binder, catalyst AS-8209-18-30 was formulated with a nickel oxide-silica co-precipitate that had been previously soaked in a potassium carbonate solution. The test results also showed a lower catalytic activity than that of catalyst AS-8209-6-13 (19).

In order to determine the effect of an alkaline earth metal dopant, catalyst AS-8209-24-33 was formulated with a nickel oxide-silica-barium oxide co-precipitate, and bonded with a barium hydroxide-gelled silica. The test results showed a far lower catalytic activity than that of catalyst AS-8209-6-13 (19).

In order to determine the effectiveness of lithium as a dopant, catalyst AS-8209-26-26 was formulated with a lithium oxide-doped nickel oxide-silica co-precipitate, and bonded with a lithium hydroxide-gelled silica. These test results also showed a lower catalytic activity than that of catalyst AS-8209-6-13 (19).

The three catalysts doped with potassium (AS-8209-18-30), barium (AS-8209-24-33), and lithium (AS-8209-26-26) incorporated all or part of their dopants into their nickel oxide-silica matrix, whereas catalyst AS-8209-6-13 incorporated its sodium dopant into only its binder. In order to determine the effect

of this parameter, catalyst AS-8209-28-6 was formulated with the standard, undoped nickel oxide-silica co-precipitate, and bonded with a potassium hydroxide-gelled silica. The resulting extrudates had a potassium content which was one third that of catalyst AS-8209-18-30 . The tests results showed a catalytic activity that was comparable to that of catalyst AS-8209-6-13(20).

In order to investigate this effect further, catalyst AS-8209-32-23 was formulated with the standard, undoped nickel oxide-silica co-precipitate, and bonded with a barium hydroxide-gelled silica. The initial test results were so promising that they were extended to a 28 day, 4550 cycle run. Figure 13 shows this extended run for catalyst AS-8209-32-23, as well as the shorter runs for catalysts AS-8209-28-6 and AS-8209-6-13.

These runs show that when the dopant is added to the silica binder, long term stability is enhanced. However, catalysts prepared with no alkali or alkaline earth dopants, or catalysts prepared with the dopant added to the nickel oxide-silica co-precipitate, have faster deactivation rates and higher carbon build-ups.

The least squares fit shown in Figure 13 for the barium-doped catalyst AS-8209-32-23 indicated that the methane production rate might level out to a 2.05 ml CH_4/gm cycle asymptote, thus negating the need for regenerating a commercial catalyst bed which was sized for the asymptotic methane production rate. Naturally, such long term extrapolation of such limited data is risky. Furthermore, the 26.5 wt.% of residual inactive carbon found on the catalyst after the last cycle was in poor agreement

FIGURE 13

LONG TERM DEACTIVATION RUNS FOR DOPED SILICA-MATRIXED CATALYSTS

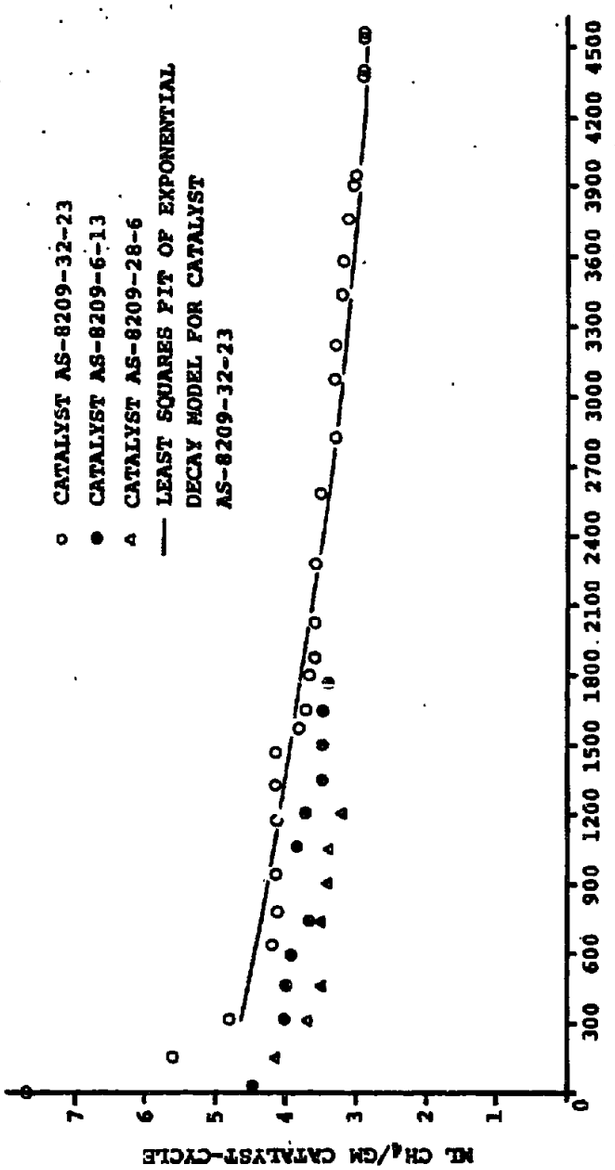

with the <0.35 wt.% residual inactive carbon levels found for catalysts AS-8209-28-6 and AS-8209-6-13 at the end of their somewhat shorter runs.

It is obvious that additional catalyst development runs would have to be made to define more fully the extent of the inactive carbon formation and the true asymptotic value of the methane production rate for this, and other similarly doped catalysts, before Phase II of the COthane program could begin.

VI REACTOR STUDIES

A study of reactor configurations for the COthane process requires a consideration of the thermodynamic equilibrium limitations of the reactions and the amount of heat released during each step of the process(4). Table XVI shows that if the active carbon is assumed to have a thermodynamic activity half way between that of graphite and that of an active carbon described by Dent(24), as was indicated by the experimental data, then both steps of the COthane process can be expected to go nearly to completion over the 270-300°C operating range for a feed stream containing only CO as a reactant. Furthermore, Table XVII shows that under these conditions the total amount of heat released over the entire cycle will be ~80 kilocalories/4 gram moles of reacted CO, and that if the thermodynamic activity of the active carbon is half way between that of graphite and dent carbon, the 80 kilocalorie heat release will be made up of a 57 kilocalorie heat release from the disproportionation step and a 23 kilocalorie heat release from the steaming step.

These heat releases can pose two problems. They can cause an unacceptably high temperature rise to occur in the reactor during any one of the COthane steps, thus favoring the formation of a less active, more graphitic carbon, and they can cause heat to accumulate over the course of each cycle. Consequently, any reactor design considered for COthane service must be able to moderate the temperature rises and insure that all heat released during each complete cycle is removed from the reactor prior to the beginning of the next cycle. Figure 14

TABLE XVI TABULATION OF K_p FOR REACTIONS (I), (II), AND (III) BETWEEN 200°C-340°C WITH GRAPHITE AND DENT (3) CARBON

$$4CO \rightleftharpoons 2C^* + 2CO_2 \quad \text{(I)}$$

$$2C^* + 2H_2O \rightleftharpoons CH_4 + CO_2 \quad \text{(II)}$$

$$4CO + 2H_2O \rightleftharpoons CH_4 + 3CO_2 \quad \text{(III)}$$

°C	°K	GRAPHITE K_p (I)	(II)	(III)	DENT CARBON K_p (I)	(II)
200	473	0.44306E+20	0.68846E-01	0.30503E+19	0.20133E+11	0.15151E+09
220	493	0.12366E+19	0.79076E-01	0.97787E+17	0.79797E+10	0.12254E+08
240	513	0.45596E+17	0.89707E-01	0.40902E+16	0.30502E+10	0.13410E+07
260	533	0.21530E+16	0.10066	0.21672E+15	0.11328E+10	0.19131E+06
280	553	0.12678E+15	0.11187	0.14183E+14	0.41144E+09	34470.
300	573	0.90991E+13	0.12326	0.11215E+13	0.14695E+09	7632.1
320	593	0.78033E+12	0.13478	0.10517E+12	0.51868E+08	2027.7
340	613	0.78594E+11	0.14637	0.11504E+11	0.18170E+08	633.13

TABLE XVII

TABULATION OF ΔH FOR REACTIONS (I), (II), AND (III) BETWEEN 200°C-340°C WITH GRAPHITE AND DENT (3) CARBON

Heat of Reaction in Calories/gm. moles as written

$$4CO \rightleftharpoons 2C^* + 2CO_2 \qquad (I)$$

$$2C^* + 2H_2O \rightleftharpoons CH_4 + CO_2 \qquad (II)$$

$$4CO + 2H_2O \rightleftharpoons CH_4 + 3CO_2 \qquad (III)$$

		GRAPHITE			DENT CARBON	
°C	°K	(I)	(II)	(III)	(I)	(II)
200	473	-82963.	3231.8	-79731.	-20122.	-59609.
220	493	-82980.	3191.4	-79789.	-22834.	-56955.
240	513	-82990.	3151.5	-79839.	-25569.	-54270.
260	533	-82993.	3112.2	-79881.	-28319.	-51563.
280	553	-82989.	3073.7	-79916.	-31073.	-48842.
300	573	-82979.	3036.1	-79942.	-33824.	-46119.
320	593	-82961.	2999.5	-79962.	-36561.	-43401.
340	613	-82938.	2964.0	-79974.	-39276.	-40698.

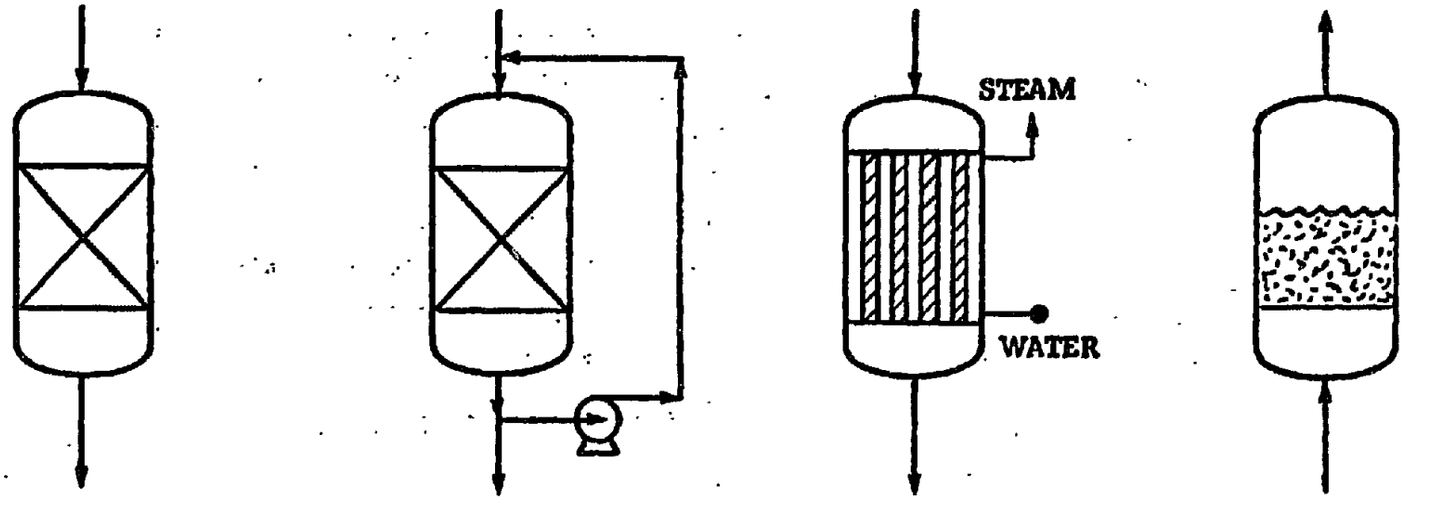

CASE I
FIXED BED
ONCE-THROUGH

CASE II
FIXED BED
WITH RECYCLE

CASE III
TUBULAR REACTOR
WITH HEAT REMOVAL

CASE IV
FLUIDIZED BED

FIGURE 14

REACTOR CONFIGURATIONS

shows the four commonly used reactor configurations that were studied from the view of controlling the temperature rise and ensuring complete heat dissipation.

HEAT EFFECTS IN ADIABATIC PACKED BED REACTORS

Cases I and II in Figure 14 are adiabatic packed bed reactors, whose operation are characterized by the movement of separate mass and heat transfer fronts down the length of the bed. The relative speeds of the fronts determine the maximum temperature rise that occurs in the bed, as well as the positions of the temperature fronts when the mass front has nearly reached the end of the bed at the end of a cyclic step.

Figure 15 illustrates the situation when the heat front travels faster than the reaction-cooling front. As the reaction-cooling front moves forward, the inert components in the gas passing through it pick up the heat of the reaction, carry this heat forward, ahead of the reaction-cooling front, as sensible heat, and then transfer it back to the cooler portion of the bed, downstream from the reaction-cooling front. The net result is a slow moving reaction-cooling front separated from a more rapidly moving heating front by an expanding region of constant temperature heat storage. This region expands until it reaches the end of the bed, at which point the heat front passes out of the bed. Moreover, when the slower moving reaction-cooling front reaches the end of the bed, usually at the end of a process step, most of the bed will be at the temperature of the feed gas. Thus, under these circumstances the heat of the

FIGURE 15

TEMPERATURE PROFILE WHEN THE HEATING FRONT MOVES FASTER THAN THE REACTION FRONT

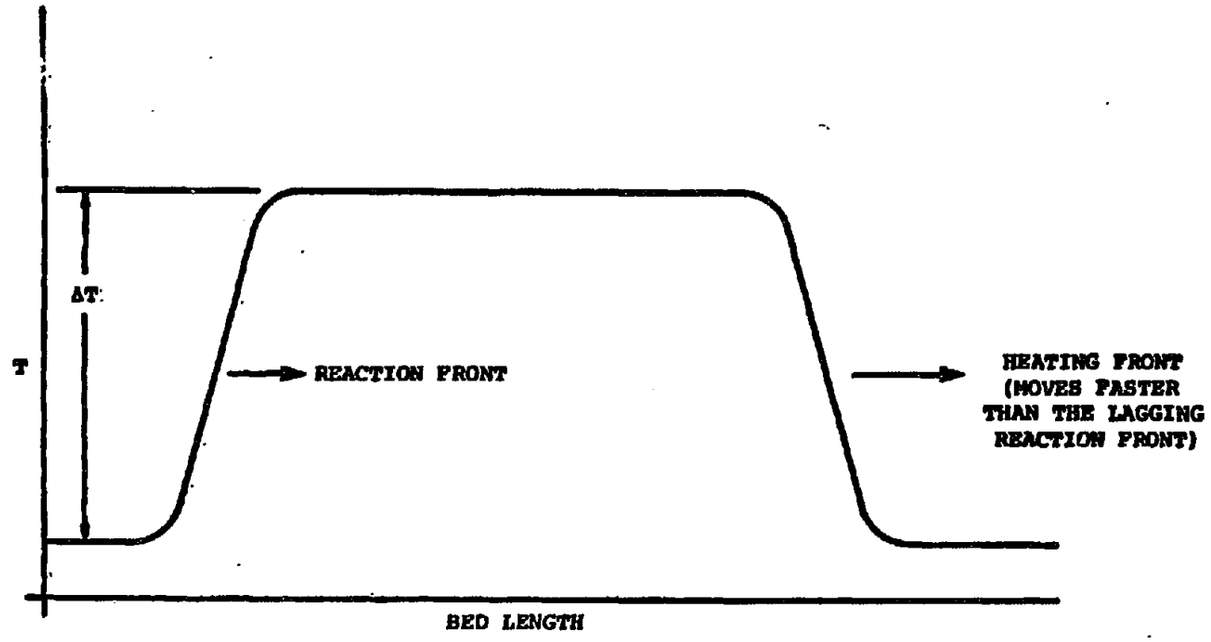

reaction, and any residual latent heat in the bed, will have been flushed from the bed by the end of the cycle step(4).

Figure 16 illustrates the situation when the reaction-heating front travels faster than the cooling front. As the feed gas passes through the slower-moving cooling front, it picks up sensible heat from the bed and passes on to the leading reaction-heating front. As the hot gas moves through the front, the sensible heat of the gas and the heat of reaction are used to heat up the bed ahead of the front. Consequently, by the end of the cycle, when the reaction-heating front has reached the end of the bed, the portion of the bed between this front and the cooling front will be at some higher temperature than that of the feed gas. Moverover, no heat will have been flushed from the bed(4).

Which of the front distributions shown in Figures 15 and 16 will actually occur during each of the COthane process steps will depend on the values for the heat capacity of the gas stream, the heat capacity of the catalysts, the mole fraction of CO in the stream, Y, and the active carbon loading of the catalyst, X (4). The actual temperature rise occurring in the bed between the two temperature fronts will additionally depend on the bulk density of the bed and the heat of reaction(4). Figure 17 shows the bed temperature rise occuring during the disproportionation step as a function of the mole fraction of CO with a catalyst having an assumed 1 wt.% loading of either graphite or Dent carbon. Figure 18 shows a similar relationship

FIGURE 16

TEMPERATURE PROFILE WHEN THE REACTION FRONT MOVES FASTER THAN THE COOLING FRONT

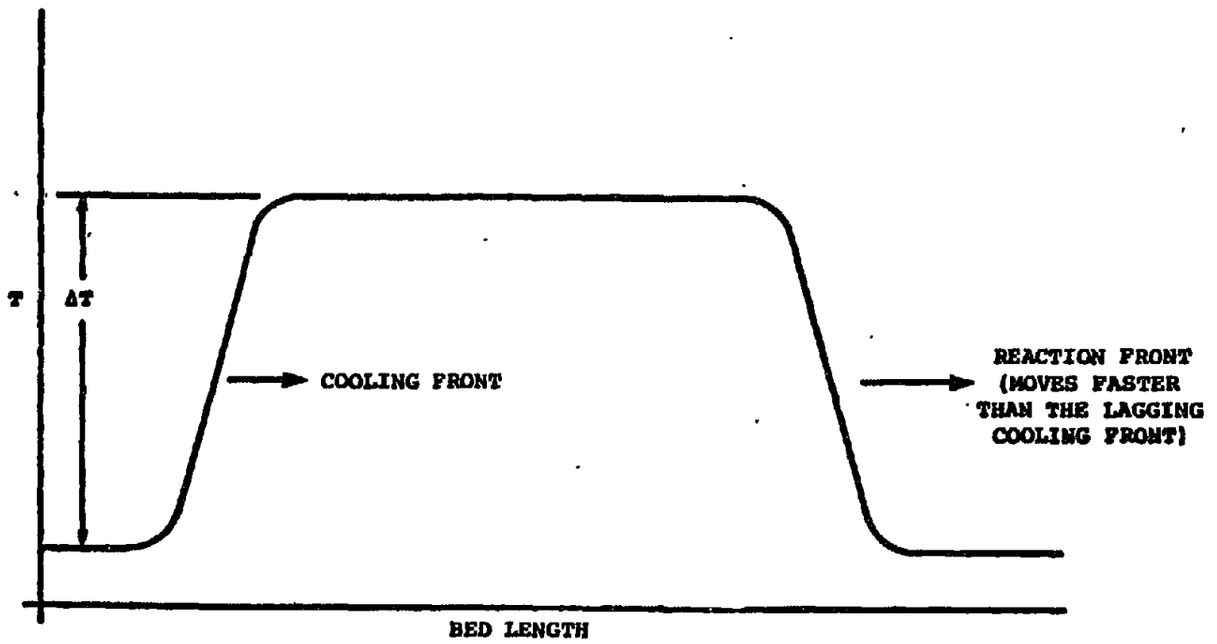

FIGURE 17

THE ADIABATIC BED TEMPERATURE RISE AS A FUNCTION OF INLET CO CONCENTRATION DURING THE DISPROPORTIONATION STEP

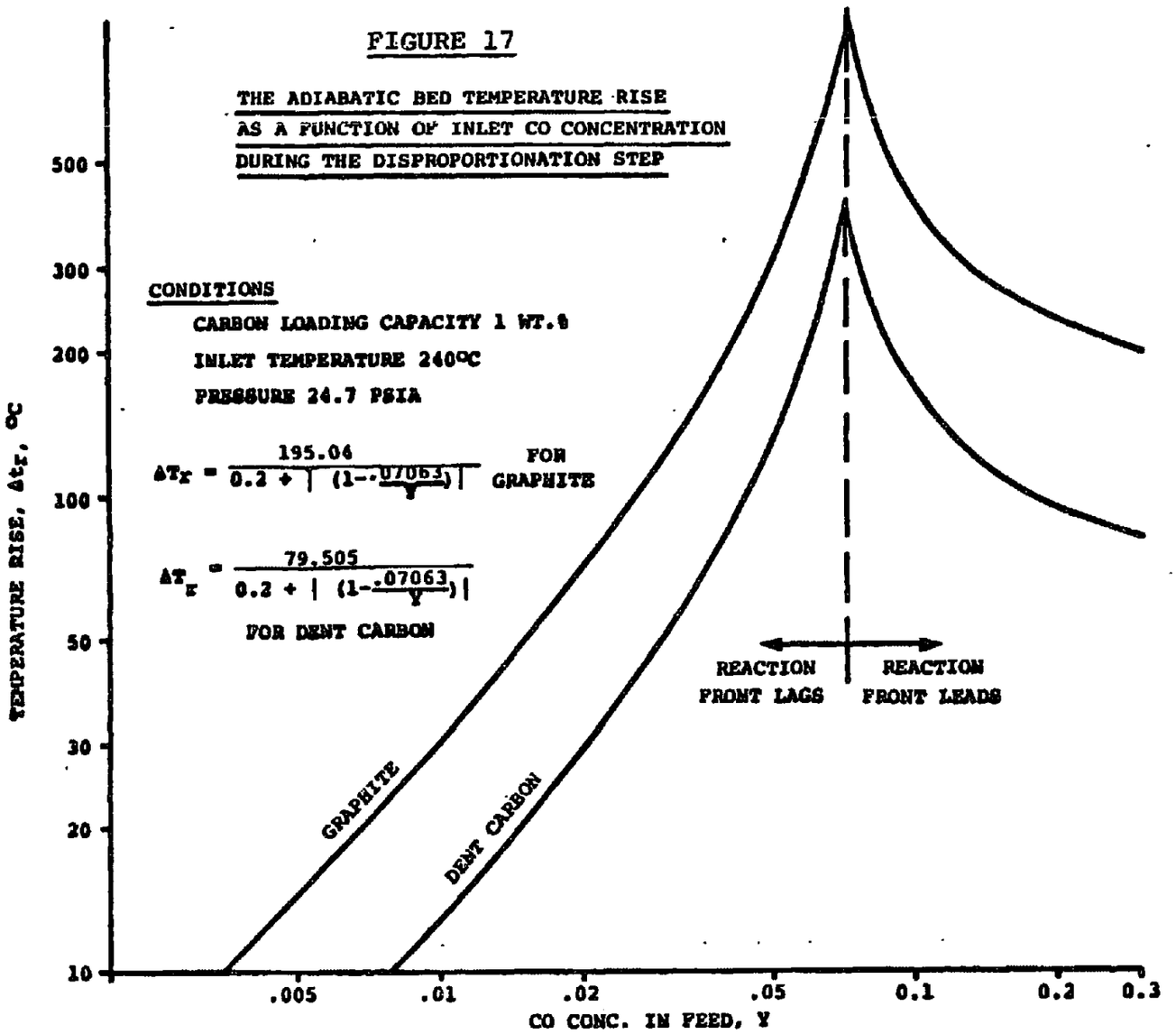

FIGURE 18

THE ADIABATIC BED TEMPERATURE RISE
AS A FUNCTION OF THE INLET CONCENTRATION
DURING THE STEAMING STEP FOR DENT CARBON

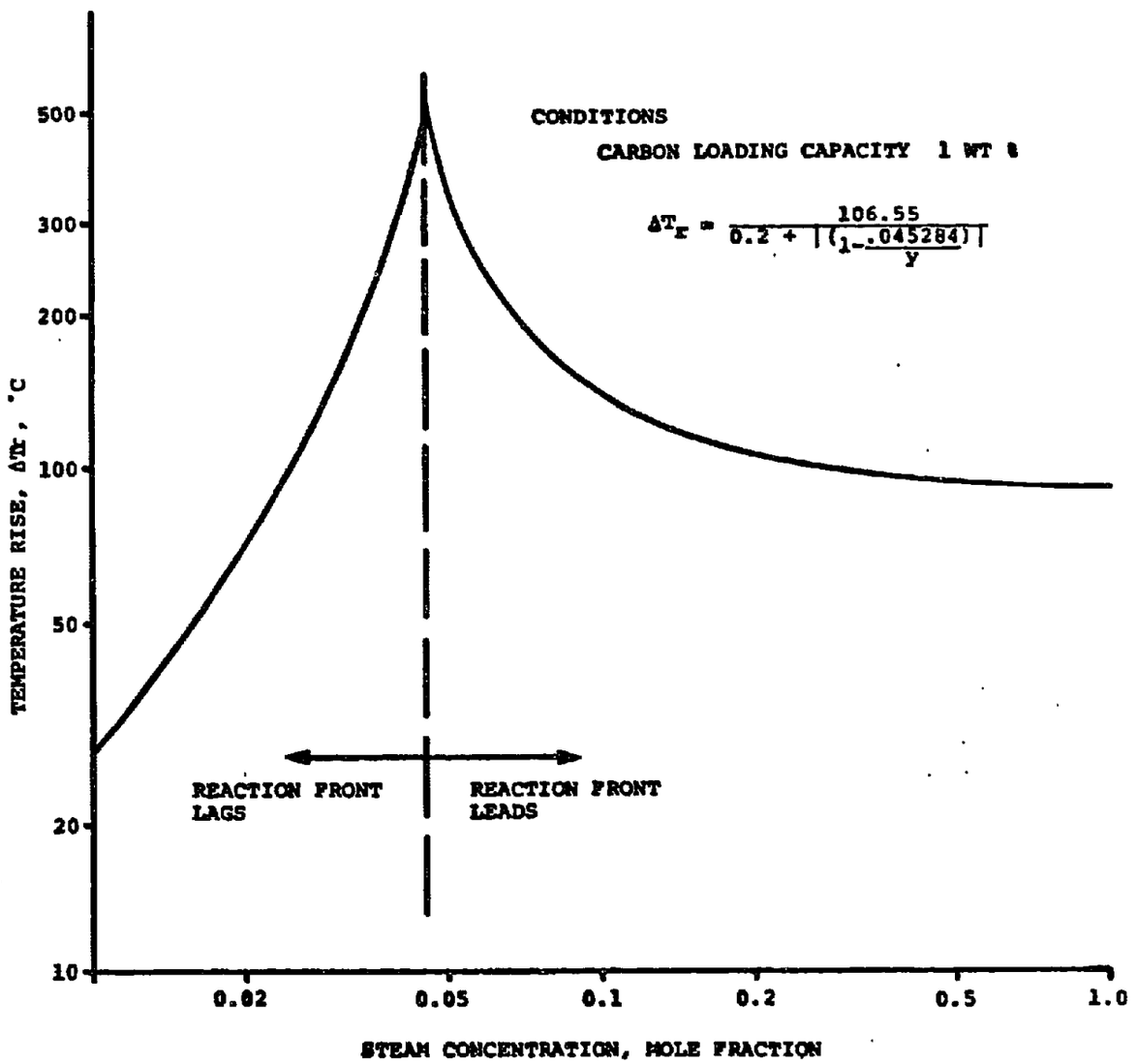

for the steaming step. In each of these figures, the curve lying to the left of the peak represents the temperature rises that will occur in the bed as the reaction-cooling front lags behind the heat front. Similarly, the curve lying to the right of the peak represents the bed temperature rises that will occur as the reaction-heating front leads the cooling front. If the active carbon loading is less than 1.0 wt.%, the curves are similar, but are displaced to the left.

If a feed gas containing ~25 mole% CO, such as blast furnace off-gas, is fed to an adiabatic reactor, Figure 17 shows that the reaction-heating front will lead, so that when this process step ends and the reaction-heating front is at the end of the bed, no heat will have left the reactor, and a portion of the bed will be at a higher temperature, ΔT_r, than the feed gas temperature. Figure 18 shows that the same thing will happen during the steaming step, when 100% steam is introduced into the bed. It thus can be seen that unless the bed is cooled with a purge gas at the end of each process step, the generated heat will accumulate in the bed from step to step until the cumulative rise in the bed temperature will prevent further cycling.

However, if the feed gas is sufficiently diluted with recycled effluent gas, Figure 17 indicates that the reaction-cooling front will lag behind the heating front, so that when this process step is over and the reaction-cooling front is at the end of the bed, all of the heat that was released during this step, and all of the heat that was released and left behind

in the bed from the previous steaming step, will have been swept out of the bed. Because operating the disproportionation step with diluted feed gas removes the heat released from both steps, there is no cumulative heat build-up, and the cycle can be run repeatedly.

The amount of diluent mixed with the feed gas will depend on the size of the temperature rise that can be tolerated in the bed. This temperature rise can be no larger than the difference between the maximum temperature at which the catalyst can operate with an acceptably low inactive carbon formation rate and the lowest temperature at which the active carbon formation will proceed at a desirably fast rate. This lower temperature is usually called the initiation temperature and is the feed inlet temperature. The initiation temperature for the COthane catalyst is ~240°C and the optimum upper temperature is ~300°C. Consequently, ΔT_r is ~60°C. Figure 17 indicates that for a 60°C ΔT_r and a 1 wt.% loading of an active carbon having a heat of reaction half way between that of graphite and Dent carbon, the feed gas must be diluted to the extent that the mole fraction of CO will be ~0.022. Similarly, Figure 18 indicates that the temperature rise during the steaming step, with the use of pure steam, will be ~100°C, 40°C higher than would be desirable. However, if the loading of active carbon on the catalyst were only 0.5 wt.%, which is more in line with the catalysts developed to date, a 60°C temperature rise during the disproportionation step would require a 0.017 mole fraction of CO entering the reactor, and the

steaming step would cause a 53°C bed temperature rise.

These calculations show that a straight through adiabatic packed bed reactor, such as that shown for Case I of Figure could effectively handle the heat loads of the COthane process if the CO feed concentration were low. However, if the CO feed concentration were high, then either the bed would have to be purged between process steps, or the inlet gas would have to be diluted, presumably by recycled effluent gas as is shown for Case II of Figure 14.

HEAT EFFECTS IN A COOLED, PACKED BED TUBULAR REACTOR

The heat generated in a packed bed reactor can also be dissipated through radial conduction, when the catalyst is placed in many paralled tubes surrounded by a cooling medium, as shown for Case III of Figure 14. Consequently, a mathematical model(27), describing such dissipation of heat fronts in packed bed reactors, was used to anticipate what would happen when the COthane cycle was run with a high concentration feed gas(7).

Figure 19 shows the calculated bed temperature rises as a function of the tube length and the overall heat transfer coefficient, U, with a 2" diameter tubular reactor, a 0.5 wt.% active carbon loading, a 1 foot long reaction front, a 0.275 CO mole fraction, and an eight minute step time, when the reaction front has reached the end of the reactor at the end of the disproportionation step. It can be seen that when U=0, the bed is adiabatic and the temperature fronts are disposed in the same way as was shown in Figure 16 for the case where the reaction-heating front preceeds the lagging cooling front.

FIGURE 19

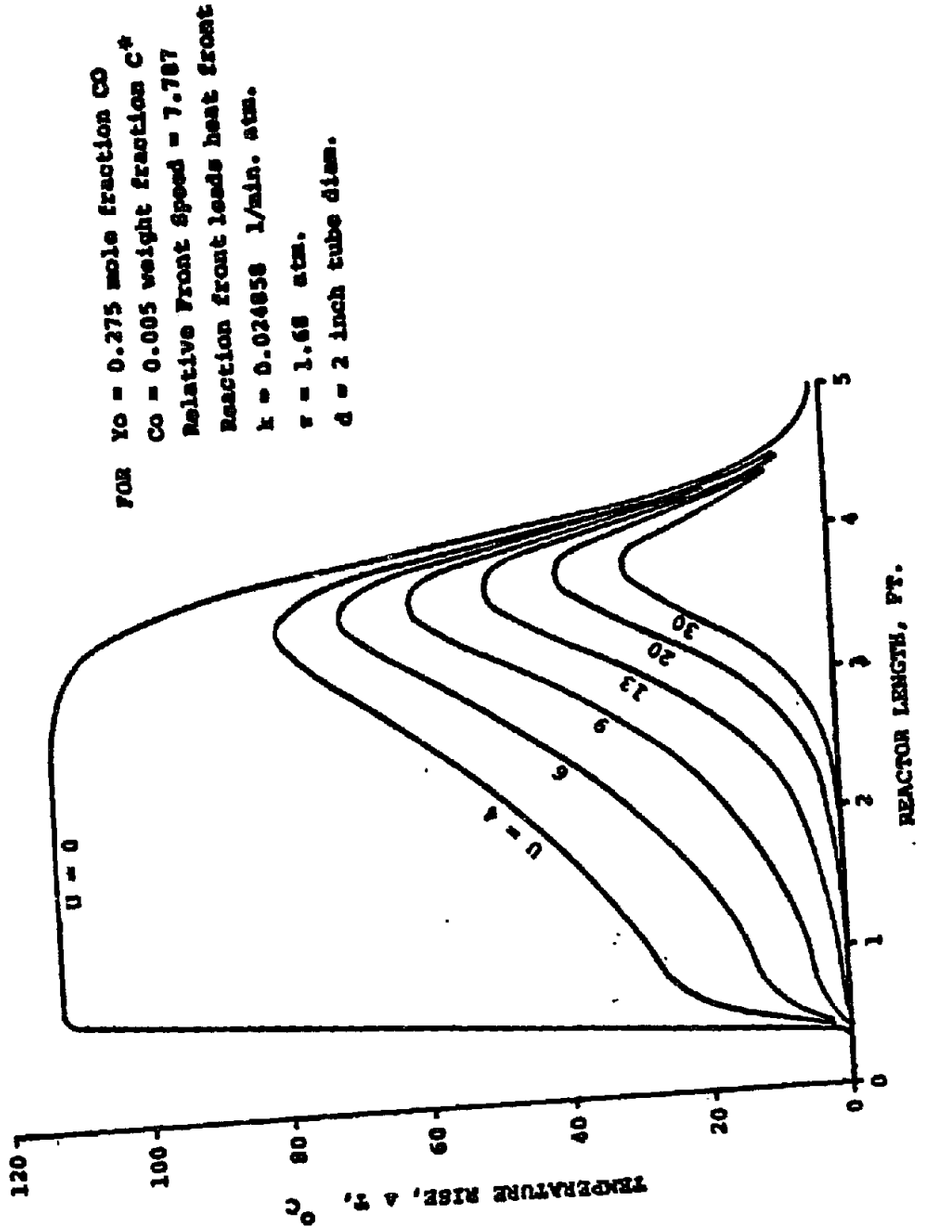
TEMPERATURE RISE IN A TUBULAR REACTOR WITH HEAT REMOVAL
FOR Yo = 0.275 mole fraction CO
Co = 0.005 weight fraction C*
Relative Front Speed = 7.787
Reaction front leads heat front
k = 0.024858 1/min. atm.
r = 1.68 atm.
d = 2 inch tube diam.
U = 0
U = 4
6
9
13
20
30
TEMPERATURE RISE, Δ T, °C
REACTOR LENGTH, FT.
0
20
40
60
80
100
120
0
1
2
3
4
5

However, when U>0, the bed is no longer adiabatic and the heat profile becomes skewed. Figure 19 indicates that the temperature rises have dropped to their lowest values at the entrance of the bed, which has had the longest time to dissipate heat, and for systems with the highest overall heat transfer coefficients. Similar plots for different tube diameters also illustrated the expected decrease of the temperature rise with a decrease of tube diameter(7). Furthermore, the maximum temperature rise occurring at the reaction-heating front can be expected to be smaller with a longer reaction zone, where there is more tube surface area available to dissipate the heat as it is formed. Similarly, the residual temperature rises remaining at the beginning of the bed at the end of a cycle step can be expected to be smaller with longer step times, when there is more time for the heat to dissipate.

The actual shape of the temperature profile for a given tube diameter, overall heat transfer coefficient, molar gas flux, and process step time will depend on the actual length of the reaction zone. Both reaction zone lengths and resulting temperature profiles were found from the mini PDU reactor runs described in Chapters III and IV.

During the complete COthane cycle, each of the two steps causes its own reaction-heating front to move down the length of the reactor tube. By the time this front has reached the bottom of the reactor tube, the top of the tube has cooled and is ready for the next reaction-heating front of the next cycle step. The cycle operates continuously in this manner with the

heat fronts from the two steps sequentially rippling down the length of the tube. The diameter of the reactor tubes and the temperature of the Dowtherm coolant are such that the peak temperature rise occurring at the reaction-heating front is within acceptable limits, and all of the reaction heat is dissipated through the tube walls over the course of each cycle.

HEAT EFFECTS IN A FLUIDIZED BED REACTOR

The heat of reaction can also be removed with a fluidized bed reactor, as indicated by Case IV of Figure 14. While the catalyst charge in this fluidized bed reactor is in a turbulent, fluidized state, it is never removed from the reactor. As was the case for the packed bed reactors, there are two fluidized beds, and the feed and steam streams are alternatively switched back and forth between them in a cyclic manner. The fluidized state of the catalyst charge results in a uniform operating temperature throughout the bed. The heat of reaction is removed from the bed through submerged cooling coils, similar to those envisioned for fluidized combustion beds.

The reactor will be operated in a fluidized-bed mode for the disproportionation step, and in a settled, fixed-bed mode for the low flux steaming step(9). During the fixed bed operation of the steaming step, when the submerged cooling coils become ineffective, the reaction-heating front will lead the cooling front, the heat of reaction will remain within the bed as sensible heat, and the bed temperature between the leading and lagging

fronts will rise from ~250°C to ~300°C. During the subsequent fluidized bed operation of the disproportionation step, when the submerged cooling coils become effective, the temperature profile will disappear, both the sensible heat accrued during the steaming step and the heat of the disproportionation reaction will dissipate through the cooling coils, and the bed temperature will drop from ~300°C to ~250°C. This cycle will repeat itself continuously, with both the direct removal of the heat of the disproportionation reaction and the indirect removal of the heat of the steaming reaction occuring during the disporportionation step.

The primary disadvantage of a fluidized bed reactor is that the catalyst must have a high resistance to attrition, a requirement which would necessitate a catalyst development program which was beyond the scope of the one envisioned for this contract. Furthermore, because of the gas by-passing that intrinsically occurs in fluidized beds, as much as 10% of the CO present in the feed gas could pass through the bed unreacted.

VII ECONOMIC STUDIES

PRELIMINARY ECONOMIC STUDY

The reactor studies showed that the temperature rises associated with the COthane process for most potential feed streams can be controlled either by recycling effluent feed gas around an adiabatic packed bed reactor, by feeding the undiluted feed gas directly into a tubular reactor, or by feeding undiluted feed gas directly into a fluidized bed reactor. These three cases were evaluated (8) early in the program with assumed design parameters for the treatment of a typical quantity of blast furnace off-gas.

This preliminary study showed that the tubular reactor case had the lowest capital and production costs. The adiabatic bed case required a prohibitively expensive recycle compressor, while the fluidized bed case required a reactor that was at least as expensive(13) as the tubular reactor, a lower CO utilization, and an attrition resistant catalyst.

In light of these initial flindings, the efforts of the experimental studies were directed towards measuring CO utilizations, active carbon loadings, and reactor zone lengths for a tubular reactor. Once these design numbers were measured, they were used in a final, more comprehensive economic study.

FINAL ECONOMIC STUDY

Table I shows that 77% of all recoverable waste CO is present in the off-gases of the blast, basic oxygen, and carbon black furnaces. Consequently, COthane process economics were examined for all three of these cases in accordance with the tubular reactor design data obtained over the course of the program. This design data was translated into the following major assumptions:

- The COthane cycle time is 1½ minutes, with the disproportionation and the pressurization/steaming/depressurization steps each taking 45 seconds apiece.
- The reactor tubes are 1" in diameter.
- The catalyst will last 1 year. During this service life the active carbon loading will not fall below 0.2 wt.% and the reaction zone length will not extend beyond 7 feet.
- The CO utilization is 20% for the blast furnace off-gas and basic oxygen off-gas cases, and 25% for the carbon black off-gas case.
- All feed streams are dehydrated prior to their being sent to the COthane reactor. H_2S is also removed from the carbon black gas, but hydrogen is not.

Additional process and economic assumptions, as well as the feed compositions and the component parts of the methane production costs, are given in Tables XVIII through XXIV for the three different feed streams. The costs were calculated in conformance to the procedures laid down in an ESCOE report (22), with the exception that there is no provision for off-sites, such as buildings, paving, utilities and other auxiliaries needed for an automonomous plant. Such off-sites are assumed to be available at any of the plants that would be using the COthane process to upgrade their waste gases. Furthermore, the feed gases for the COthane process were assumed to be previously flared off-gases, which had no use to the user, and consequently a zero value for the study.

Figure 20 shows the flow diagram for a COthane unit handling 15.7 MMSCFD of blast furnace off-gas. It is similar to those for the COthane units handling the basic oxygen and carbon black off-gases. During the disproportionation step the blast furnace off-gas passes through a dehydrator, an influent/effluent heat exchanger, a ZnO guard bed, a trim preheater, and onto the reactor. During the steaming step 100-150 psig steam passes through a preheater and into the reactor; the reaction products pass through a carbon dioxide removal unit, a final dehydrator, and onto the local natural gas pipeline distribution system.

TABLE XVIII

DESCRIPTION OF THE OFF-GASES USED FOR THE COthane ECONOMIC STUDIES

DESCRIPTION	BLAST FURNACE OFF-GAS	BASIC OXYGEN FURNACE OFF-GAS	CARBON BLACK OFF-GAS
Gas Flow (STP = 60°F and 14.7 psia)	15.7 MM SCFD	4.68 MM SCFD	22.9 MM SCFD
Gas Pressure	14.7 PSIA	14.7 PSIA	14.7 PSIA
Gas Temperature	100°F	100°F	100°F
Composition (dry basis)			
CO, % by volume	27.5	10-70% (40% of time)	15.0
CO_2, % by volume	10.0	Balance	3.3
H_2, % by volume	3.0		15.0
N_2, % by volume	58.0		66.5
O_2, % by volume	1.0	1-2%	---
CH_4, % by volume	0.5		---
H_2S, % by volume	---		0.2
TOTAL	100.0	100.0	100.0
Water Content	Saturated	Saturated	Saturated

TABLE XIX

PROCESS AND ECONOMIC ASSUMPTIONS USED FOR THE ECONOMIC STUDY OF THE COthane PROCESS HANDLING BLAST FURNACE OFF-GAS

A. PROCESS ASSUMPTIONS

1. Feed gas compression from 14.7 psia to 36 psia is required to pass through the downstream equipment.

2. The feed gas contains less than 1 ppm of sulfur-containing compounds.

3. The feed gas is sent to a glycol dehydrator after it is compressed to 36 psia.

4. The feed gas leaving the COthane reactor is heat-exchanged with the influent stream.

5. The feed gas passes through a ZnO guard bed.

6. The reactor consists of a shell and tube heat exchanger with the catalyst packed inside the 1" tubes and Dowtherm vapor generated on the shell side.

7. The process is a two step (disproportionation and steaming steps), two bed process. Each step takes 45 seconds.

8. Each 11.2 foot long reactor tube includes a 4.2 foot long equilibrium section, corresponding to a 0.2 wt.% loading of active carbon, and a 7 foot long reaction zone section. The pressure drop across the reactor is less than 13.5 psi.

9. The 11.2 foot long, 1" OD reactor tubes are grouped together into two sets of shell and tube reactors, each set consisting of four reactors and containing 47,493 lbs. of catalyst. These two sets of reactors are alternatively used for the two steps of the COthane process. Since the catalyst needs to be regenerated only during normal shutdowns, there is no need for a third set of reactors for continual, on-going regenerations.

10. The catalyst is assumed to have a one year life. Over this length of time the cumulative lengthening of the adsorption and reaction sections will not exceed 11.2 ', so that the CO front will always remain within the reactor tubes.

11. Boiling Dowtherm is used to cool the tubes down to 250-270°C and generate 500 psig steam in a separate reboiler. The maximum temperature within the catalyst tubes does not exceed 310°C.

12. The steaming step uses twice the stoichiometric amount of steam required for this reaction. The excess steam assures the high pressure displacement of the CH_4 and CO_2 from the bed. The residual steam depressurized from the bed supplies any additional heat required by the Benfield (CO_2 removal) unit; however, the exact heat integration of the Benfield unit will need further study.

13. In order to prevent capillary condensation, the steaming step is carried out at $\leq$150 psig.

14. The entering 240°C feed gas contains 27.5% CO, which causes the reaction front to precede the cooling front, as is the case for the steaming step. Both of these heat rises are moderated by the radial heat removal through the walls of the 1" reactor tubes. In effect, each step causes a heat/reaction front to ripple down the length of the reactor. By the time the front has reached the bottom of the reactor tube, the top of the tube has cooled and is ready for the next heat/reaction wave. The heat removed from the tubes during these steps generates 500 psig steam through the intermediate use of boiling Dowtherm on the shell side of the reactor.

15. After the disproportionation step, each bed is purged with atmospheric CO_2, which is recycled from the Benfield unit, to displace the feed gas remaining in the void spaces. The bed is then sealed off and pressurized with steam as part of the steaming step. Thermodynamics indicate that at the 250-310°C bed temperatures there should be negligible quantities of CO formed from the reversal of the disproportionation reaction (i.e., $CO_2 + C^* \rightleftharpoons 2CO$).

16. In each case the effluent from the steaming step is sent to the Benfield unit which yields a 225°F water-saturated stream containing 97% CH_4 and 3% CO_2 (dry basis). This stream is cooled to 100°F, separated from its condensate, and sent to the glycol dehydrator. The pipeline quality gas leaving the dehydrator contains less than the specified 147 ppm of water.

B. ECONOMIC ASSUMPTIONS

1. All major equipment is fabricated out of carbon steel.

2. The feed gas, which would normally be flared, is priced at $0/MMSCF.

3. The cost estimates for the feed and product glycol dehydrators were supplied by the Chemicals and Plastics Research and Development Department.

4. The cost estimate for the Benfield unit was supplied by the Benfield Corporation.

5. The cost estimate for the tubular reactor was 5% above the bid received from a supplier who consistently submitted the lowest, but reasonable, bids for similar 3/4" diameter tube reactors.

6. The cost estimate for the influent/effluent heat exchanger was obtained from Econotherm.

7. The cost estimates for most of the remaining items of equipment were obtained from Guthrie (23).

8. The equipment costs were scaled up to installed costs by using suitable knock-up factors.

9. When the utility charges were costed as follows:

Cooling water	$0.05/MGAL
Power	$0.03/KWH
Steam	
15-20 psig	$1.75/MLBS
50 psig	$2.50/MLBS
300 psig	$3.50/MLBS
600 psig	$3.76/MLBS

The total utility debits and credits were found to cancel each other out, or yield a small positive credit (21). Consequently, for the sake of simplicity the overall utility costs were given an arbitrary zero value.

10. The purchase cost of the catalyst is $4.00/lb. The catalyst has a one year life.

11. Labor is costed at $12/operator and $20/supervisor. An additional 40% charge is used to cover all fringe benefits.

12. All costs are based on the second quarter of 1980, with the Marshall and Stevens index being 650.7.

13. There are 346 stream days/year.

TABLE XX

PROCESS AND ECONOMIC ASSUMPTIONS USED FOR THE ECONOMIC STUDY OF THE COthane PROCESS HANDLING BASIC OXYGEN FURNACE OFF-GAS

A. PROCESS ASSUMPTIONS

The process assumptions are the same as those given for the blast furnace off-gas case (see Table XIX), with the following modifications:

- There is a sufficient number of basic oxygen furnaces to insure a continuous source of off-gas to the COthane unit. The CO concentration in the off-gas, which varies over twenty minute cycles, starts out from 10 vol.%, rises to a maximum 70 vol.%, stays at 70 vol.% for eight minutes, and then drops rapidly back down to 10 vol.%. The COthane reactors are designed to handle the 70 vol.% peak CO concentration.

- Each 14.7 foot long reactor tube includes a 7.7 foot long equilibrium section, corresponding to a 0.2 wt.% loading of active carbon, and a 7 foot long reaction zone section. The pressure drop across the reactor is less than 11 psi.

B. ECONOMIC ASSUMPTIONS

The economic assumptions are the same as those given for the blast furnace off-gas case (see Table XIX), with the following modifications:

- Equipment costs were adjusted from the costs found for the blast furnace off-gas study. The size exponent varied from 0.6 to 1.0, depending on the particular piece of equipment.

- The total utility debits and credits were assumed to balance out, as was found for the blast furnace off-gas study.

TABLE XXI

PROCESS AND ECONOMIC ASSUMPTIONS USED FOR THE ECONOMIC STUDY OF THE COthane PROCESS HANDLING CARBON BLACK OFF-GAS

A. PROCESS ASSUMPTIONS

The process assumptions are the same as those given for the blast furnace off-gas case (see Table XIX), with the following modifications:

- The hydrogen is not removed from the off-gas, despite is thermodynamic potential for reducing all of the active carbon as it is formed. The CO utilization was assumed to be the 25% value found in the mini PDU studies.
- The H_2S is removed from the off-gas via dehydration and adsorption. This route appeared to be more economical than using an amine system.
- Each 9.4 foot long reactor tube includes a 2.4 foot long equilibrium section, corresponding to a 0.2 wt.% loading of active carbon, and a 7 foot long reaction zone section. The pressure drop across the reactor is less than 12.5 psi.

B. ECONOMIC ASSUMPTIONS

The economic assumptions are the same as those given for the blast furnace off-gas case (see Table XIX), with the following modifications:

- Equipment costs were adjusted from the costs found for the blast furnace off-gas study. The size exponent varied from 0.6 to 1.0, depending on the particular piece of equipment.
- The total utility debits and credits were assumed to balance out, as was found for the blast furnace off-gas study.

TABLE XXII

INSTALLED COSTS FOR THE COthane UNITS HANDLING THREE DIFFERENT OFF-GASES

SPECIFICATION	INSTALLED COSTS, MID-1980 DOLLARS		
	BLAST FURNACE OFF-GAS	BASIC OXYGEN FURNACE OFF-GAS	CARBON BLACK OFF-GAS
Feed Supply System:			
Compressor system	$ 543,500	$ 230,500	$ 974,800
Dehydrator	317,800	153,700	398,600
H_2S removal system	---	---	785,500
Reactor System:			
Influent/effluent H.E.	208,900	101,100	270,200
ZnO Guard bed	23,500	11,400	38,100
Preheater	98,900	47,900	127,900
Tubular reactors(2)	2,424,800	1,516,500	3,054,300
Dowtherm reboiler	282,400	136,600	365,200
Methane Treatment System:			
CO_2 removal unit	490,100	301,900	422,400
Condenser	45,200	21,900	56,700
Dehydrator	46,700	28,800	40,200
Regeneration System:			
Heat exchanger	5,900	3,100	7,600
Heater	16,200	7,700	20,100
Compressor	47,600	22,900	59,600
ROV's	100,000	100,000	100,000
TOTAL	$4,651,500	$2,684,000	$6,721,200
Size adjustment factor:	0.92	0.95	0.90
TOTAL INSTALLED COST	$4,279,400	$2,549,800	$6,049,100

TABLE XXIII

WORKING CAPITAL COSTS FOR THE COthane UNITS HANDLING THREE DIFFERENT OFF-GASES

IN MID-1980 DOLLARS

	BLAST FURNACE OFF-GAS	BASIC OXYGEN FURNACE OFF-GAS	CARBON BLACK OFF-GAS
CATALYST	$ 379,900	$ 256,600	$ 435,400
DOWTHERM	125,400	85,800	136,400
TETRAETHYLENE GLYCOL	9,900	7,100	14,400
MOLECULAR SIEVE	---	---	251,500
ZnO	9,900	7,100	14,400
TOTAL	$ 525,100	$ 356,600	$ 852,100

TABLE XXIV

CHEMICALS AND CATALYST COSTS FOR THE COthane UNITS HANDLING THREE DIFFERENT OFF-GASES IN MID-1980 DOLLARS

	CHEMICALS & CATALYST COSTS		
	BLAST FURNACE OFF-GAS	BASIC OXYGEN FURNACE OFF-GAS	CARBON BLACK OFF-GAS
CATALYST (1 YR. LIFE)	$ 379,900	$ 256,600	$ 435,400
DOWTHERM	6,300	4,300	6,800
TETRAETHYLENE GLYCOL	5,000	3,600	7,200
MOLECULAR SIEVE (3 YR. LIFE)	---	---	83,800
ZnO	5,000	3,600	7,200
TOTAL	$ 396,200	$ 268,100	$ 540,400

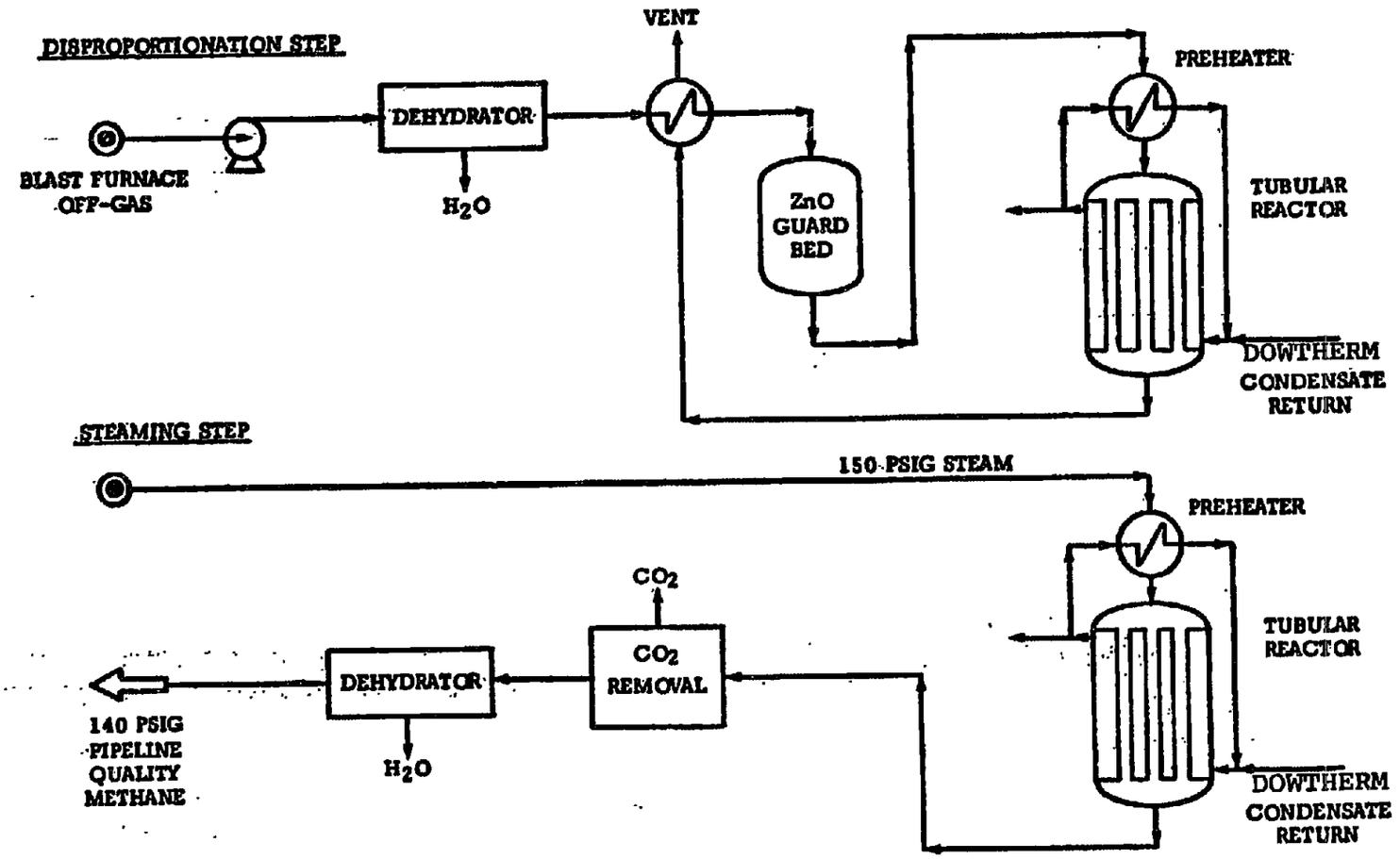

FIGURE 20

THE COTHANE PROCESS HANDLING BLAST FURNACE OFF-GAS WITH TUBULAR REACTORS

Table XXV shows that the COthane methane production costs (in mid-1980 dollars) for the three feed streams are $5.78/MM BTU for the blast furnace off-gas, $7.11/MM BTU for the basic oxygen furnace off-gas, and $8.10/MM BTU for the carbon black off-gas. The cost for the basic oxygen furnace off-gas is higher than the cost for the blast furnace off-gas because the reactor handling the basic oxygen off-gas has to accommodate a peak CO concentration. The cost for the carbon black off-gas is higher than the cost for the blast furnace off-gas becuase the additional treatment step is required to remove the H_2S in the carbon black gas, and because larger supporting equipment is needed to handle the larger quantity of the more dilute carbon black gas, even though the reactor costs and the total methane production rates are nearly the same for the two cases.

The cost of producing methane from carbon black off-gas could be reduced from $8.10/MM BTU to $6.00/MM BTU by first removing the hydrogen from the feed stream, and then using that hydrogen in place of steam during the steaming, or hydrogenating, step of the COthane cycle. The larger capital costs required for hydrogen removal is more than off-set by the higher CO utilization obtained when hydrogen is used as the hydrogenating agent (20).

These costs are significantly higher than the $2-4/MM BTU cost of natural gas today, and are significantly higher than the $5.07 MM/BTU estimated (19) present cost of SNG produced by the Lurgi process. However, this gap between the COthane production costs and the other fuel costs can be expected to eventually narrow, disappear, and then reverse itself with time,

TABLE XXV

PRODUCTION COSTS FOR THE COthane UNITS HANDLING THREE DIFFERENT OFF-GASES IN MID-1980 DOLLARS

	BLAST FURNACE OFF-GAS	BASIC OXYGEN FURNACE OFF-GAS	CARBON BLACK OFF-GAS
I. CAPITAL COSTS[1]			
Total Installed cost	$4,279,400	$2,549,800	$6,049,100
Contingency @ 20%	855,900	510,000	1,209,800
Working Capital	525,100	356,600	852,100
Total Capital Cost (TCC)	$5,660,400	$3,416,400	$8,111,000
II. OPERATING COSTS			
Chemicals and catalyst	$ 396,200/yr.	$ 268,100/yr.	$ 540,400/yr.
Utilities (net)	-0-	-0-	-0-
Labor (1 man, 1/4 sup.)	191,800	191,800	191,800
Maintenance (3% of TCC)	169,800	102,500	243,300
Local taxes and insurance (5% of TCC)	283,000	170,800	405,600
Total Operating Cost	$1,040,800/yr.	$ 733,200/yr.	$1,381,100/yr.
III. CAPITALIZED COST (PRIVATE FINANCING)			
(0.115)(TCC)	$ 650,900	$ 392,900	$ 932,800
IV. HEATING VALUE OF PRODUCED METHANE/YR.	292,771 MM BTU/yr.	158,368 MM BTU/yr.	285,641 MM BTU/yr.
V. METHANE PRODUCTION COST $\frac{\text{(OPERATING COST + CAPITALIZED COST)}}{\text{(HEATING VALUE)}}$ =	$ 5.78 MM BTU/yr.	$ 7.11/MM BTU	$ 8.10/MM BTU

(1) The capital cost does not include off-sites.

since the COthane costs will rise only with the costs of materials and labor, which, in turn, are expected to increase more slowly than fuel costs (including the cost of coal required for the Lurgi process).

The gap between the COthane production costs and the other fuel costs might also be decreased by improving the life and performance of the catalyst. Figures 21, 22, and 23 indicate that if a catalyst were to be developed with a two year life, a 0.4 wt.% final active carbon loading, and a 3½ foot maximum reaction zone length, the methane production costs would drop to $3.65/MM BTU for the blast furnace off-gas, $4.45/MM BTU for the basic oxygen furnace off-gas, and $5.50/MM BTU for the carbon black off-gas. Furthermore, if the hydrogen in the blast furnace off-gas were first removed, and then used as the hydrogenating agent, the methane production cost would drop to $4.00/MM BTU. All of these costs assume that the resulting higher heat fluxes could still be dissipated with 1" reactor tubes. An additional $0.33-$0.61/MM BTU saving could be realized by halving the one man year labor costs; however, this saving would require justification based on commercial experience.

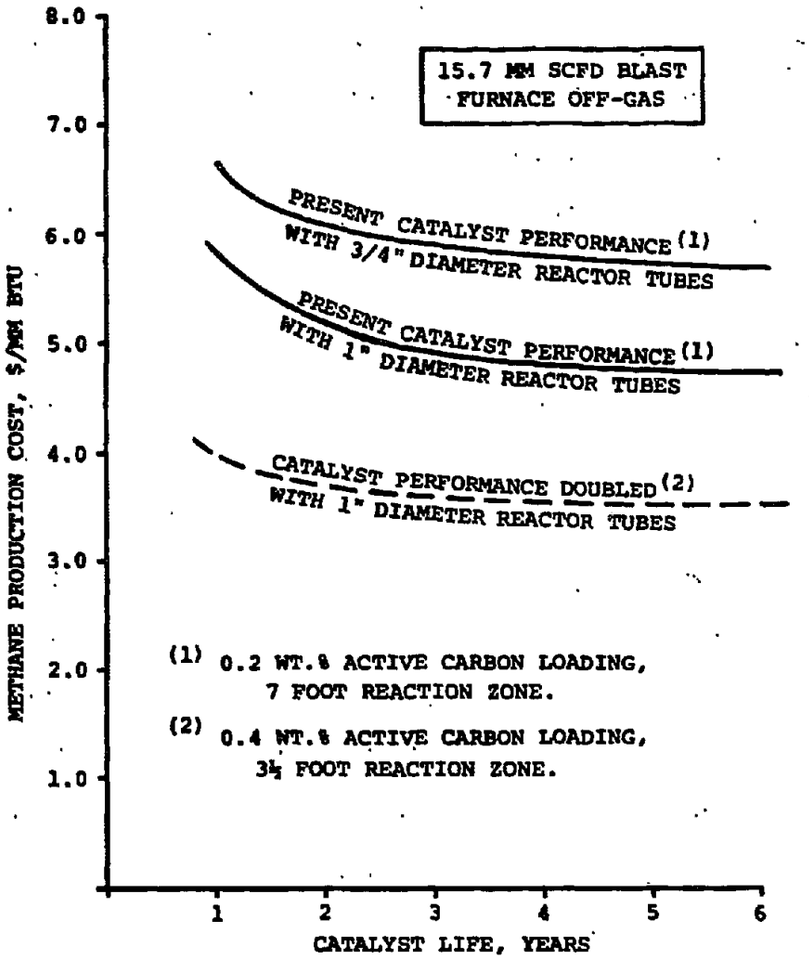

FIGURE 21

METHANE PRODUCTION COSTS AS A FUNCTION OF CATALYST PERFORMANCE, CATALYST LIFE, AND REACTION TUBE DIAMETER FOR A COthane UNIT HANDLING 15.7 MM SCFD OF BLAST FURNACE OFF-GAS IN MID-1980 DOLLARS.

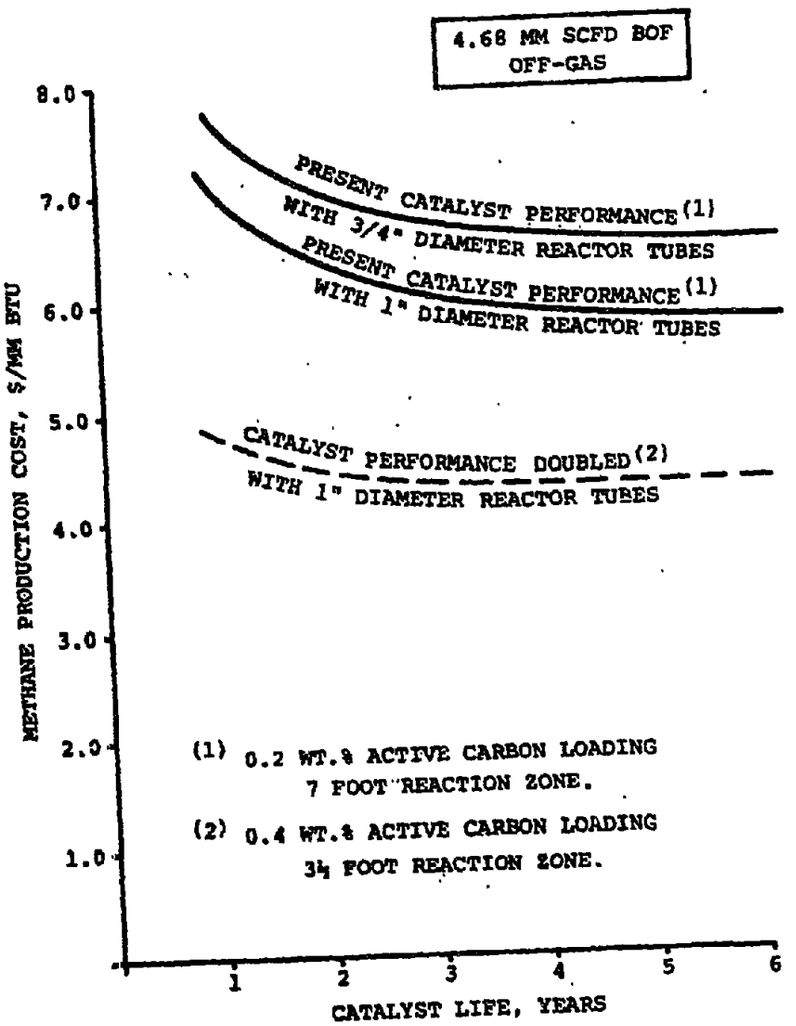

FIGURE 22

METHANE PRODUCTION COSTS AS A FUNCTION OF CATALYST PERFORMANCE, CATALYST LIFE, AND REACTOR TUBE DIAMETER FOR A COthane UNIT HANDLING 4.68 MM SCFD OF BOF OFF-GAS IN MID-1980 DOLLARS.

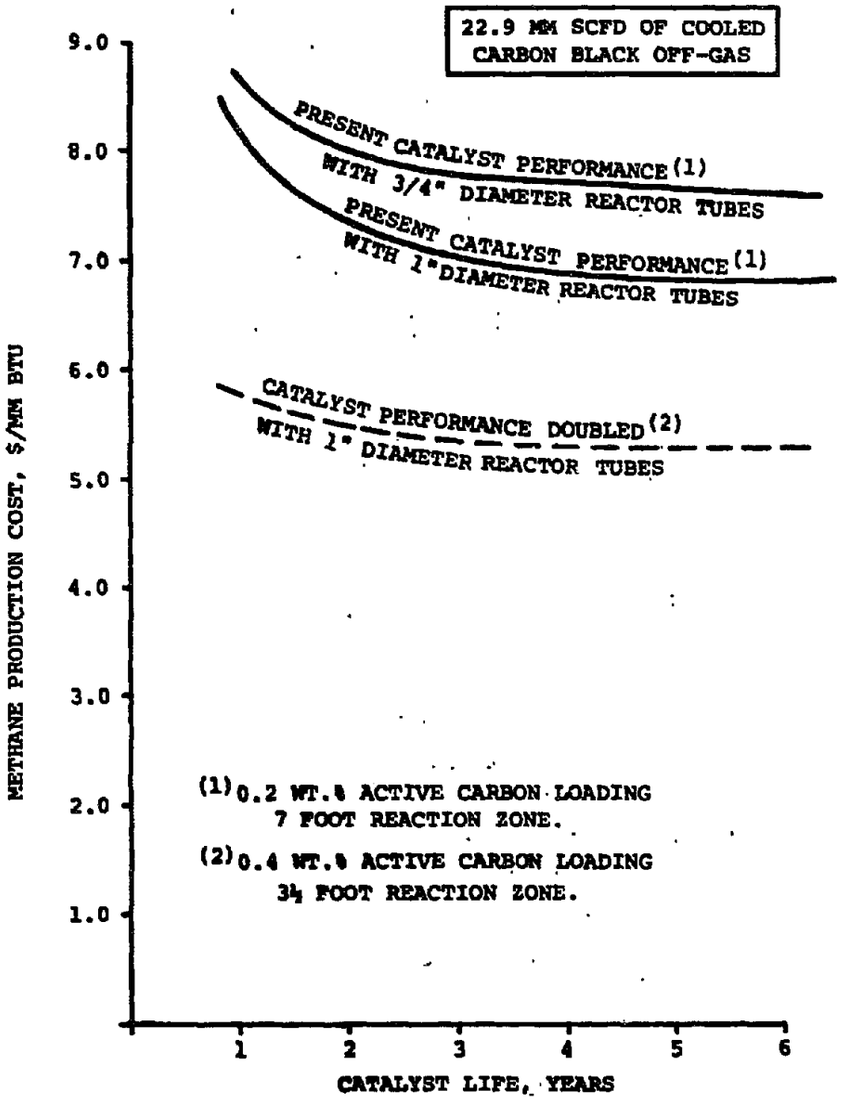

FIGURE 23

METHANE PRODUCTION COSTS AS A FUNCTION OF CATALYST PERFORMANCE, CATALYST LIFE, AND REACTOR TUBE DIAMETER FOR A COthane UNIT HANDLING 229 MM SCFD OF COOLED CARBON BLACK OFF-GAS IN MID-1980 DOLLARS.

MARKET SURVEYS

Market surveys were made in the steel, carbon black, and aluminum industries. Responses from four major steel makers indicated almost full utilization of their blast furnace off-gas, and thus no need for the COthane process. However, there was interest in the use of the COthane process for handling BOF off-gas.

Responses from two major carbon black manufactures, comprising ~2/3 of the market, indicated little interest, either becuase they are assured of a cheap source of natural gas for the next 4-5 years, or because they now burn their off-gas to produce steam for across-the-fence customers.

Responses from two major aluminum manufacturers indicated that the COthane process could be used only if highly impractical modifications were made on the hoods enclosing the anodes of their prebaked cells. Since this is an industry-wide problem, no other aluminum manufacturers were surveyed.

VIII FUTURE EFFORT

Because the COthane production cost is presently above that of prevailing natural gas prices, all work on the COthane program has been suspended. However, because the cost of the COthane process will increase less rapidly than the cost of the fuel, and because a reasonable increase in catalyst performance will have a significant effect on reducing COthane costs, an additional catalyst development effort would be appropriate at some future time when fuel costs have risen substantially above their present levels.

Such an additional catalyst development effort would preceed the Phase II pilot plant studies and would concentrate on the more commercially promising basic oxygen furnace off-gas and carbon black off-gas applications.

IX BIBLIOGRAPHY

1. Unsolicited Proposal, "Methane Production from Waste Carbon Monoxide", Union Carbide Corporation, May, 1978.

2. Proprietary Data for the Cost and Management Plans of the COthane Contract No. EM-78-C-03-215, January, 1979. (Unpublished)

3. Proprietary Technical Status Report for the COthane Contract (EM-78-C-03-2153) for the Month of January, 1979. (Unpublished)

4. Proprietary Technical Status Report for the COthane Contract (EM-78-C-03-2153) for the Month of February, 1979. (Unpublished)

5. Proprietary Technical Status Report for the COthane Contract (EM-78-C-03-2153) for the month of March, 1979. (Unpublished)

6. Proprietary Technical Status Report for the COthane Contract (DE-AC03-78CS40177) for the Month of April, 1979. (Unpublished)

7. Proprietary Technical Status Report for the COthane Contract (DE-AC03-78CS40177) for the Month of May, 1979. (Unpublished)

8. Proprietary Technical Status Report for the COthane Contract (DE-AC03-78CS40177) for the Month of June, 1979. (Unpublished)

9. Proprietary Technical Status Report for the COthane Contract (DE-AC03-78CS40177) for the Month of July, 1979. (Unpublished)

10. Proprietary Technical Status Report for the COthane Contract (DE-AC03-78CS40177) for the Month of August, 1979. (Unpublished)

11. Proprietary Technical Status Report for the COthane Contract (DE-AC03-78CS40177) for the Month of September, 1979. (Unpublished)

12. Proprietary Technical Status Report for the COthane Contract (DE-AC03-78CS40177) for the Month of October, 1979. (Unpublished)

13. Technical Status Report for the COthane Contract (DE-AC03-78CS40177) for the Month of November, 1979. (Unpublished)

14. Technical Status Report for the COthane Contract (DE-AC03-78CS40177) for the Month of December, 1979. (Unpublished)

15. Interim Technical Status Report for the COthane Contract (DE-AC03-78CS40177), December, 1979.

16. Technical Status Report for the COthane Contract (DE-AC03-78CS40177) for the Month of January, 1980. (Unpublished)

BIBLIOGRAPHY
(continued)

17. Technical Status Report for the COthane Contract (DE-AC03-78CS40177) for the Month of February, 1980. (Unpublished)

18. Technical Status Report for the COthane Contract (DE-AC03-78CS40177) for the Month of March, 1980. (Unpublished)

19. Technical Status Report for the COthane Contract (DE-AC03-78CS40177) for the Month of April, 1980. (Unpublished)

20. Technical Status Report for the COthane Contract (DE-AC03-78CS40177) for the Month of May, 1980. (Unpublished)

21. Technical Status Report for the COthane Contract (DE-AC03-78CS40177) for the Month of June, 1980. (Unpublished)

22. Technical Status Report for the COthane Contract (DE-AC03-78CS40177) for the Month of July, 1980. (Unpublished)

23. Leva, M., Ind. Eng. Chem., 39, 857 (1947).

24. K. A. Rogers, R. F. Hill, "Coal Conversion Comparisons" FE-2468-51, The Engineering Societies Commission on Energy Inc. (ESCOE), prepared for the United States Department of Energy under Contract No. EF-77-C-01-2468, July, 1979.

25. K. M. Guthrie, "Process Plant Estimating, Evaluation, and Control", Craftsman Book Company of America, Solana Beach, California, 1974.

26. F. J. Dent, L. A. Mognard, A. H. Eastwood, W. H. Blackburn, D. Hebden, 49th Report of the Joint Research Committee, The Gas Research Board, London, England, 1945.

27. B. M. Johnson, G. F. Froment, C. C. Watson, Chem. Eng. Science, 17, 835-845, (1965).

28. J. J. Collins, Chemical Engineering Progress Symposium Series No. 74, "The LUB/Equilibrium Section Concept For Fixed Bed Adsorption".

29. L. Seglin, "Methanation For Synthesis Gas", Advances in Chemistry Series 146, ACS, Washington, D.C. 1975.

30. J. A. Rabo, A. P. Risch, and M. L. Poutsma, Journal of Catalysis, 53, No. 3, 295-311, July, 1978.

BIBLIOGRAPHY
(continued)

31. C. A. Rohrman, P. M. Molton, D. C. Elliott, C. T. Li, E. G. Baker, G. F. Schiefelbein, "Interim Report on Study of Energy Conservation by Chemical Production Using Carbon Monoxide From Industrial Waste Gases", Battelle Pacific Northwest Laboratories, November 1, 1976.

32. Private communication from Professor J. W. Geus.

33. U.S. Patent Application 889,558, "Methanation of Carbon Monoxide Without Prior Separation of Inert Cases".

APPENDIX I

ESTIMATION OF THE NICKEL SURFACE AREA

1. 1 wt.% active surface carbon (ASC) per gram catalyst.

2. Assume ASC = 1 C atom per surface nickel atom.

3. 1 nickel atom = 6.5×10^{-20} m^2 (area occupied).

4. 1 gm catalyst loads 0.01 gm ASC (see 1 above).

5. $0.01\ \text{gm ASC} = 8.3 \times 10^{-4} \frac{\text{mole ASC}}{\text{gm catalyst}} = 8.3 \times 10^{-4} \frac{\text{mole Ni (surface)}}{\text{gm catalyst}}$

6. $8.3 \times 10^{-4} \frac{\text{mole Ni (surface)}}{\text{gm catalyst}} \times 6.023 \times 10^{23} \frac{\text{Ni atom}}{\text{mole Ni}} \times$

   $6.5 \times 10^{-20} \frac{m^2\ \text{Ni}}{\text{Ni atom}} = \frac{32.5\ m^2\ \text{Ni}}{\text{gm catalyst}}$

   1 wt.% ACS requires ~32 $\frac{m^2\ \text{Ni}}{\text{gm catalyst}}$

7. A typical nickel catalyst particle of 15 nm that is fully exposed has a calculated surface area of ~45 m^2 Ni/gm nickel, consequently a catalyst would have to be ~70% nickel at ~15 nm to have 32 m^2 Ni/gm catalyst surface area.

APPENDIX II

SUMMARY OF THE TECHNIQUES USED TO SYNTHESIZE COTHANE CATALYSTS

I. TECHNIQUE A

The slow decomposition of urea at 90°C in a solution of dissolved salts slowly raises the solution pH, and thus slowly precipitates out the hydrous oxides (32).

EXAMPLE: Catalyst AS-5005-3-25 was prepared by dissolving 81.38 grams of zirconyl nitrate, 465.7 grams of nickel nitrate, and 351 grams of urea into 1100 cc. of distilled water preheated to 90°C. This solution was contained in a 5 liter, round bottom flask, equipped with an overhead stirrer, a heating mantel, a temperature controller set at 90°C, and a pH meter. The slow hydrolysis of the urea, $(NH_2)_2\,CO + 3H_2O \xrightarrow{90^\circ C} 2NH_4^+ + 2OH + CO_2$, caused the solution pH to rise from 1.8 to 5.7 over a period of 4 hours, and finally reach 6.4 after 24 hours. The co-precipitate of hydrous oxides that slowly formed from this slow climb in pH was filtered from the solution, washed with distilled water, dried at ~100°C, and extruded with 10-15 wt.% peptized alumina to 1/16" extrudates. These extrudates were air-calcined at 480°C and then reduced with a 5 vol.% H_2/95 vol.% N_2 mixture at 400°C.

II. TECHNIQUE B

The slow injection of NaOH into a solution of dissolved salts slowly raises the solution pH, and thus slowly precipitates out the hydrous oxides (32).

EXAMPLE: Catalyst AS-5005-71-8 was prepared by dissolving 50 grams of zirconyl nitrate and 727.5 grams of nickel nitrate into 5 liters of distilled water, which was contained in a 12 liter, round bottom flask equipped with an overhead stirrer. A separate NaOH solution, made from 240 grams of sodium hydroxide dissolved in 5 liters of distilled water, was slowly fed, at 2-5 ml/minute, into the well-stirred nickel-zirconyl salt solution. The co-precipitate of hydrous oxides that slowly formed from this slow addition of base was filtered from the solution, washed to remove the excess sodium hydroxide, and subsequently formulated in a manner similar to that described for Technique A.

III. TECHNIQUE C

The rapid addition of NaOH to a solution of dissolved salts rapidly raises the solution pH, and thus rapidly precipitates out the hydrous oxides.

EXAMPLE: Catalyst Material AS-8209-2 was prepared by dissolving 2792 grams of nickel nitrate and 250 grams of AS-40 Ludox colloidal silica into 6.5 liters of distilled water. A separate NaOH solution, made from 920 grams of sodium hydroxide dissolved in 10 liters of distilled water, was added as rapidly as possible to the well-stirred nickel-silica solution. The co-precipitate of hydrous oxides that quickly formed from this rapid addition of base was filtered from the solution, washed to remove the excess sodium hydroxide, and subsequently formulated in a manner similar to that described for Technique A.

*U.S. GOVERNMENT PRINTING OFFICE: 1981-740-145/2225